MASTERARBEIT | MASTER'S THESIS

Titel | Title

Exploring how stamen morphology changes across elevation and pollination systems in Merianieae (Melastomataceae)

verfasst von | submitted by

Fabian Polz BSc

angestrebter akademischer Grad | in partial fulfilment of the requirements for the degree of

Master of Science (MSc)

Wien | Vienna, 2025

Studienkennzahl lt. Studienblatt | Degree programme code as it appears on the student record sheet:	UA 066 832
Studienrichtung lt. Studienblatt | Degree programme as it appears on the student record sheet:	Masterstudium Botany
Betreut von | Supervisor:	Ass.-Prof. Agnes Dellinger BSc MSc PhD

Abstract (Deutsch)

Die Tribus Merianieae (Melastomataceae) hat unterschiedliche Strategien zur Optimierung des Pollentransfers evolviert, indem sie auf Bestäuber variierender Qualität und Quantität setzt. In höheren Lagen haben extremere abiotische Bedingungen zu einer Verschiebung von Vibrationsbestäubung durch Bienen hin zu Bestäubung durch Sperlingsvögel oder gemischte Vertebratengruppen (z. B. Kolibris, Fledermäuse, Nagetiere) geführt. Bienen, die in tiefen Lagen häufig, in höheren jedoch seltener vorkommen, werden als Bestäuber geringer Qualität betrachtet, da sie Pollen primär als Futter ihrer Larven sammeln. Im Gegensatz dazu sind fruchtkörperverzehrende Sperlingsvögel und nektarfressende Vertebraten qualitative Bestäuber, da sie große Mengen Pollen mit geringen Verlusten transferieren. Mit Bestäuberverschiebungen gehen Veränderungen in Bestäuberbelohnungen und Pollenverbreitungsstrategien einher, die sich in angepassten Staubblattmerkmalen manifestieren.

Mittels vergleichender morphometrischer Analysen untersuchte ich die Anpassungen der Staubblätter entlang von Höhengradienten sowie in Abhängigkeit von Bestäuberqualität, -quantität, sowie Pollendosierungsmechanismen. Durch Computertomographie-(CT)-Scans an Staubblättern von 69 Merianieae-Arten erfasste ich quantitativ mittels der Software Amira die wesentlichen Merkmale (Antherenlänge, Anhängselvolumen, Konnektivvolumen, Porengröße und Thekenvolumen). Durch phylogenetische lineare Regressionsanalysen und Hauptkomponentenanalyse untersuchte ich, wie sich die Staubblattmorphologie in Reaktion auf Bestäubungssysteme und Höhenlage verändert.

Sperlingsvogel-bestäubte Arten weisen signifikant größere Konnektivanhängsel auf, was auf die Evolution der Fruchtkörperbelohnung und explosiven Pollenfreisetzung rückzuführen ist. Arten, die von gemischten Vertebratengruppen bestäubt werden, zeigen Trends zu größeren Poren sowie erhöhtem Konnektiv- und Thekenvolumen, was Anpassungen an das gemischte Vertebraten-Bestäubungssystem nahelegt. In bienenbestäubten Arten vergrößern sich Konnektivanhängsel, Porengrößen und Thekenvolumen signifikant mit zunehmender Höhenlage, was möglicherweise die Pollenverbreitung in Regionen mit geringer Bienendichte erleichtert.

Diese Studie liefert neue Erkenntnisse zur Evolution der Staubblattmorphologie und zu Bestäubungssyndromen in Merianieae. Der vergleichende morphometrische Ansatz stellt die erste detaillierte Quantifizierung innerer Staubblattvolumina innerhalb der Melastomataceae dar und bildet eine Grundlage für weiterführende Analysen der komplexen evolutionären Mechanismen porizider Staubbeutel.

Abstract

The tribe Merianieae (Melastomataceae) has evolved several strategies to optimize pollen transfer by relying on pollinators of varying quality and quantity. At higher elevations, harsher abiotic conditions have driven shifts from buzz-pollination by bees to passerine birds or mixed vertebrate pollinators (i.e., hummingbirds, bats, rodents). Bees, abundant at lower elevations but scarce at higher ones, forage for pollen and are thus low-quality pollinators. In contrast, fruitbody-foraging passerines and nectar-foraging vertebrates (NFV) are high-quality pollinators, transferring large amounts of pollen with little loss. Since pollinator rewarding and pollen dispersal strategies have changed concomitantly with pollinator shifts, stamen traits have also changed markedly.

Using comparative morphometric analyses, I examined stamen morphological adaptations along elevational gradients, variations in pollinator quality and quantity, and pollen dispensing mechanisms. I conducted computed tomography (CT) scans of stamens of 69 Merianieae species, measuring key traits (anther length, appendage volume, connective volume, pore size and thecal volume) with AMIRA software. I assessed how stamen morphology evolved in response to pollination systems and elevation by phylogenetic Linear Regression Models and phylogenetic Principal Component Analyses.

Passerine-pollinated species exhibit significantly larger bulbous connective appendages, indicating a shift toward food-body rewards and explosive pollen expulsion. NFV-pollinated species show trends toward larger pore size, as well as increased connective and thecal volumes, suggesting distinct adaptations for the NFV-syndrome, though these differences were not significant. Among bee-pollinated species, appendage volume, pore size, and thecal volume increase significantly with elevation, likely facilitating pollen dispersal in environments with low bee abundance.

This study provides insights into the evolution of stamen morphology and pollination syndromes in Merianieae. The comparative morphometric approach represents the first detailed quantification of internal stamen volumes within Melastomataceae and serves as a foundation for further analyses to determine the intricate evolutionary processes occurring within poricidal anthers.

Contents

Introduction

Pollinators exert selective pressure on flower traits and thus are key drivers of floral trait evolution in angiosperms (Bartkowska and Johnson 2012). The quantitative selective process is shaped by the predominant vector – the most frequent and most efficient pollinator (Stebbins 1970). Ivey et al. (2003) define efficiency or 'effectiveness' as both 'quantity' and 'quality' of a floral visitor affecting the plant's fitness and reproductive success. Whereas quantity combines frequency and abundance of a pollinator's visit (Ivey et al. 2003), Ne'Eman et al. (2010) describe the pollinator's quality as how much pollen reaches the stigma of a conspecific flower, which is determined by the pollen load on the pollinator's body, pollen loss, visit duration, and whether and how often a pollinator touches the stigma. Pollinators that transfer pollen from several conspecific individuals increase mate diversity and outcrossing, while those that deposit great pollen quantities from a single plant individuum reduce genetic variation (Mitchell et al. 2013).

According to the concept of Pollen Presentation Theory (PPT), a flower that is visited frequently by many pollinators can maximize pollen transfer to conspecific stigmas (across many different plant individuals) by reducing the amount of pollen available for pollinator pickup per visit (Percival 1955; Thomson et al. 2000). The decelerating relationship between pollen removal and pollen deposition indicates pollen wastage – how much pollen is lost during the transfer process (Harder and Thomson 1989). This led LeBuhn and Holsinger (1998) to define 'pollinator efficiency' more specifically as increasing the amount of pollen transferred while keeping the loss low (Thomson et al. 2000). Pollen loss rates from stamens to conspecific stigmas are commonly >99% (Xiao et al. 2017), which should result in plants adapting their pollen presentation schedule to the pollinator's effectiveness (Harder & Thomson 1989; Xiao et al. 2017). For example, dispensing or packaging pollen in small doses is common in animal-pollinated flowers with frequent and inefficient floral visitors (Harder & Thomson 1989; Xiao et al. 2017). Bees are both the most important pollinators worldwide and wasteful in the sense that they actively collect pollen as a food source for their brood, and hence frequently groom their bodies. This grooming behaviour reduces pollen loads on bees, causing only a few pollen grains to reach conspecific stigmas from the stigma-contacting surfaces of the bees' bodies (Castellanos et al. 2006). Furthermore, pollen is wasted when knocked to the ground or when deposited on off-target surfaces other than stigmas (Thomson et al. 2000). In contrast to pollen collecting bees, vertebrates such as hummingbirds visit flowers for nectar, lack grooming behavior and are more efficient in pollen transfer than bees. Pollen resides on a hummingbird's forehead longer than on a bee's body and is,

therefore, more likely to be transferred to the stigmas of conspecific flowers (Castellanos et al. 2006). In such cases, pollen may be dispensed more freely and in larger doses. Especially when pollinator visits are limited but have high per-visit pollen transfer rates to conspecific stigmas (low quantity – high quality), a scenario could be expected where more pollen is released at a single pollinator visit. At the other extreme, when pollinator visits are unlimited, but pollen transfer rates are low (high quantity – low quality) (Table 1), dispensing mechanisms should be favourable (Kemp and Vallejo-Marin 2021).

Table 1 Pollinator quality and quantity across pollination syndromes and altitudes; quality is based off theoretical expectations due to the foraging biology of the different pollinators (i.e., bees are scored as low-quality pollinators since they actively remove pollen grains off their bodies), quantity is based on the flower visitation behavior of 11 species according to Dellinger et al. 2021b. NFV = nectar-foraging-vertebrate; note that flower visitation frequencies of bats and rodents were low according to Dellinger et al. 2019a; since all Merianieae species studied, however, are visited by both diurnal and nocturnal pollinators and the pollinator quantity of hummingbirds is high, however, a grouped assessment of pollinator quantity should result in an overall score of "high" quantity for the NFV syndrome.

Pollinator	**Bee**	**Bee**	**Passerine**	**NFV (Bats, Rodents)**	**NFV (Hummingbirds)**
Altitude	lowland	highland	highland	highland	highland
Quality	↓ Low	↓ Low	↑ High	↑ High	↑ High
Quantity	↑ High	↓ Low	↓ Low	↓ Low	↑ High

Heteranthery, the presence of two (or more) different types of stamens, is a particularly interesting example in the context of pollen presentation theory and commonly interpreted as a strategy to counteract pollen loss (Vallejo-Marín et al. 2009). In heteranthery, stamens may differ in color, size and shape, and these combined differences may affect their attractiveness to pollinators, and, ultimately, their function in the pollination process. Accordingly, the 'division of labour' hypothesis (Darwin 1899) postulates that showy (often small) stamens function in attracting and rewarding pollinators ('feeding stamens'), while the inconspicuous (often large) stamens function in efficient pollen transfer ('pollinating stamens'). Hence, even if a pollinator consumes all the pollen from the feeding stamens, sufficient pollen from the pollinating stamens should be transferred to the pollinator's body parts that are harder to groom (H. Müller 1881, 1882; F. Müller 1883; Vallejo-Marín et al. 2009; Kemp and Vallejo-Marín 2021; Trevizan et al. 2023). The opposing selective pressure on pollen (functioning both as male gametes and as pollinator reward), is commonly regarded as evolutionary driver of heteranthery (Vallejo-Marín et al. 2009). This 'pollen dilemma' is most pronounced in

bee-pollinated, pollen rewarding flowers (i.e., no other reward provided), and, accordingly, heteranthery has evolved repeatedly in over 20 pollen-rewarding plant families (Vallejo-Marín et al. 2009; Oliveira et al. 2020; Dellinger et al. 2021a).

One pollination system which is most commonly found among pollen-rewarding flowers is buzz pollination by bees, where pollen can only be extracted from flowers through mechanical vibrations (Buchman 1983; Vallejo-Marín 2019). In buzz-pollination, bees vibrate their thoracic muscles and transmit the vibration to the stamens, resulting in a cloud of pollen expelled onto the bee's body (Buchmann 1983). Buzz pollination is widespread across an estimated 22,000 plant species across 72 families and 544 genera with varying morphology (including agriculturally important species such as tomatoes, potatoes and blueberries). A trait that is shared among many buzz-pollinated lineages, however, is that buzz-pollinated flowers typically exhibit anthers with apical pores or slits ('poricidal anthers') and dry, loose pollen as sole reward (Buchmann 1983; De Luca and Vallejo-Marín 2013). Kemp and Vallejo-Marín (2021) showed that poricidal anthers, which physically restrict access to pollen, can function as dispensing mechanism, releasing only a small proportion of pollen at the first buzz, and then increasingly smaller doses of pollen with each subsequent buzz. The ability to buzz flowers has been recorded among Apoidea within 7 families for more than 50 genera, but surprisingly not among *Apis mellifer*a (De Luca and Vallejo-Marín 2013).

With increasing elevation, abiotic environmental conditions shift towards lower temperatures, strong winds, increasing solar radiation, increasing rain, and reduction in land area (Ramos-Jiliberto et al. 2010). Therefore, mountain ecosystems are oftentimes regarded as harsh environments since organisms inhabiting these habitats are constrained physiologically (i.e., lower temperature require more energy to maintain physiological processes) and temporally (i.e., shorter growing seasons limit time for growth and reproduction; Ramos-Jiliberto et al. 2010). Accordingly, Hoiss et al. (2012) showed that species richness and abundance of wild bee communities linearly decrease with increasing elevation (but may remain high if sufficient food resources (high flower cover) are present). Especially small hymenopterans become less abundant and less diverse at higher elevations (Warren et al. 1988), as resource availability and flowering periods decrease and wind speeds, low temperatures and rain increase (Brito and Sazima 2012; Dellinger et al. 2021b). Larger insects (e.g. bumblebees, syrphid flies) that can generate heat through muscle activity, as well as larger endothermic animals such as vertebrates, however, do not only withstand these conditions but may continue visiting flowers even in light rain and at low temperatures (Lawson and Rands 2019). Accordingly, shifts from hymenopteran pollination systems in lowlands to dipteran-

dominated pollination systems at high elevations have been documented across the world (Warren et al. 1988). In the Neotropics, turnovers from bee pollination in lowlands to vertebrate pollination in montane forests are common (Dellinger et al. 2021b, 2023). Furthermore, Céspedes et al. (2022) found that the abundance of both, migratory and resident birds in the Andes, peaks at mid-elevation cloud forests and decreases with elevation. While these patterns of environment-induced turnovers in plant-pollinator interactions also suggest cascading effects on plant traits, to date, there is no detailed assessment of how pollen-dosing strategies change along elevational gradients and in light of different pollination strategies.

An ideal model system to explore pollen dosing strategies in the context of elevational gradients and different pollinator groups is the Neotropical plant tribe Merianieae (approximately 300 species) within the plant family Melastomataceae, which features both buzz-pollination by bees as well as six independent evolutionary origins of pollination by vertebrates (either passerine birds or different nectar-foraging vertebrates, Dellinger et al. 2019a). Buzz-pollinated species occur from lowland rainforests to montane environments, offering the opportunity to test for subtle differences in pollen dosing mechanisms among bee-pollinated species along climatic gradients, and hence test for the impact of the abiotic environment on stamen trait evolution. Especially in lowland tropical forests where bees are the dominant pollinators of Merianieae (Dellinger et al. 2021b), the stamens of buzz-pollinated Melastomataceae have evolved into various shapes (Castellanos et al. 2006). Bochorny et al. (2021) found that the prominent connective appendages common in the family play a functional role not only in attracting bees by visually contrasting with the colors of the petals, but also in pollen release. Specifically, stamen appendages may alter the vibrational properties of stamens, so that clipping appendages resulted in a lower pollen amount released per buzz in *Huberia bradeana* Bochorny & R.Goldenb. (Bochorny et al. 2021). These observations suggest a critical role of the stamen appendage as pollen dosing structure, making the detailed investigation of stamen appendages in an environmental context particularly important. Further, the apical pore of the tubular anthers in buzz-pollinated flowers plays an important role in limiting pollen release (Vallejo-Marín 2019). Accordingly, Dellinger et al. (2019b) found that the short and smooth ‘feeding’ stamens of the heterantherous lowland species *Adelobotrys adscendens* (Sw.) Triana had pores almost twice as large as the pores of the ‘pollinating’ stamens, allowing for easier pollen removal. The longer and corrugated ‘pollinating’ stamens, on the other hand, retained more pollen when artificially vibrated (Dellinger et al. 2019b). Given these outcomes, I expect that buzz-pollinated species visited by many bee pollinators at low elevations (low pollinator quality, high

quantity, Table 1) exhibit trait combinations that promote pollen dosing, such as long corrugated anthers with small pores and relatively small appendages. Montane bee-pollinated species, on the other hand, should have reduced pollen dosing mechanisms (short anthers with smooth walls, large pores, large appendages to facilitate grip for bees) given that they underly low pollinator quality, low quantity scenarios (Table 1).

On the flip side, in Merianieae, passerines, which can forage at harsher conditions (lower temperatures, higher windspeeds, rain), are attracted to the flowers because of the bulbous, colorful, sugary stamen appendages, which are co-opted into food bodies (Dellinger et al. 2014). The birds collect these stamen appendages and while doing so, trigger an explosive bellows mechanism and are covered in pollen (Dellinger et al. 2014). Since the birds do not actively collect pollen off their feathers and usually visit many flowers, they likely transfer pollen with higher success rates (high quality pollinators, Table 1). Smooth thecal walls are common among passerine-pollinated Merianieae and may enhance the mass ejection of pollen while dispensing mechanisms are redundant, especially as passerines pick the whole stamen out of the flower. Accordingly, passerine-pollinated species have only one shot per stamen to eject all viable pollen at once. In terms of pollinator quantity, detailed studies in two passerine-pollinated species have shown that passerines are relatively infrequent visitors (Dellinger et al. 2021a), which may lead to a scenario of high pollinator quality but low pollinator quantity (Table 1), and should hence select for reduced pollen dosing.

In contrast, Merianieae species that have shifted from bee pollination to pollination by nectar-foraging vertebrates offer nectar rewards (instead of pollen, Dellinger et al. 2019a). These species are commonly pollinated by two distinct functional groups, such as bats and hummingbirds or (more rarely) hummingbirds and rodents. Pollen release and dispensing occurs through a ‘saltshaker’ mechanism, being initiated upon contact between flower visitors and the anther’s soft thecal walls during the foraging process for nectar. In these systems, both pollinator groups can be equally effective (Dellinger et al. 2019a). Importantly, while we may assume that nectar-foraging vertebrates should be efficient pollinators that do not groom pollen grains off their bodies, they also visit flowers in high quantities (especially traplining hummingbirds, Dellinger et al. 2019a, 2021). We may thus expect moderate pollen dosing in species of this syndrome, as dosing in light of frequent pollinator visits may increase the genetic diversity of seeds (i.e., receiving pollen from multiple pollen donors).

With my Master thesis, I would like to explore how stamen morphology changes in relation to pollination systems and elevation in Merianieae. For that reason, I am

conducting morphometric analyses of stamens of 69 Merianieae species preserved in ethanol or pressed and dried from herbarium specimens.

I expect to draw conclusions on the impacts of pollinator quality and quantity in driving stamen evolution in Merianieae by studying stamen traits that are related to pollen dispensing mechanisms in Melastomataceae, i.e. anther length, appendage volume, connective volume, thecal volume, and pore size. Assuming that large thecal volumes indicate more space for pollen and that large connective appendages not only attract pollinators but also function as larger handles for larger (bee) pollinators, I expect to find larger stamens in general at higher elevations, where larger pollinators are more prevalent and require more pollen rewards. Since long but narrow anthers (with low thecal volume) may provide more space for pollen dosing through corrugated anther walls, while short anthers allow for pollen to travel a shorter distance, I expect bee-buzz-pollinated species at higher elevations (where the abundance of low-quality bee pollinators is lower) to exhibit shorter anthers with smooth thecal walls. Similarly, I am expecting that larger pores should be found among high-elevation bee-pollinated species to increase pollen release (reduced dosing). Note, however, that the relevance of the pore size regarding pollen dispensing mechanisms remains equivocal, since studies have found mixed support for the size-pollen-release relationship. Since multiple stamen traits are usually correlated, determining the decisive traits can often be challenging.

Given the overall expectations around pollinator quality and quantity (Table 1), I hypothesize that:

H1) Nectar-foraging-vertebrate- and passerine-pollinated species of Merianieae exhibit larger connective, appendage, and thecal volumes compared to bee-pollinated species, reflecting the shift to larger pollinators.

H2) Nectar-foraging-vertebrate- and passerine-pollinated species of Merianieae have larger pores and shorter anthers compared to bee-pollinated species, driven by higher pollinator efficiency and the shift to nectar and food body rewards at high elevations.

Additionally, I expect that:

H3) Lowland bee-buzz-pollinated species of Merianieae have smaller pores and longer anthers due to high pollinator quantity but low quality, whereas montane bee-buzz-pollinated species exhibit larger pores and shorter anthers, influenced by reduced pollinator quantity, and environmental conditions that restrict bee activity and hence select for reduced dispensing mechanisms.

H4) Highland bee-buzz-pollinated species of Merianieae have larger connective, appendage, and thecal volumes than their lowland counterparts, reflecting adaptations to larger montane bee pollinators.

H5) Heteranthery, as a mechanism of refined pollen placement and dispensing, is more prevalent in lowland-bee pollinated Merianieae (where bees are more common) and reflected through morphological diversity in collective, appendage or thecal volumes.

Methods

Systematics and biogeography of Merianieae

In order to obtain a representative sample of stamens of Merianieae in my thesis, I had to familiarize myself with the phylogenetic and biogeographic diversity of the tribe. I hence here provide an overview of major patterns. The tribe Merianieae encompasses eight genera distributed widely across Neotropical habitats (Figure 1, Dellinger et al. 2024), with recent phylogenetic analyses (Michelangeli et al. 2022; Penneys et al. 2022) showing polyphyletic relationships between genera and the need for taxonomic revisions To begin with, the polyphyletic *Macrocentrum* clade, consisting of 26 herbaceous species, is distributed across the Guayana Shield with few Andean species, and occurs at low (*Macrocentrum* I) to medium (*Macrocentrum* III) elevations. The monotypic *Maguiranthus* is included in *Macrocentrum* I as sister to a smaller subclade. The paraphyletic genus *Graffenrieda* (resulting from the inclusion of *Centronia laurifolia* D.Don), sister clade to *Macrocentrum* I, consists of nearly 70 shrubby (sometimes treelets) species, is predominantly distributed across the Andes and the Amazonian lowlands (Dellinger et al. 2024) and exhibits a widespread elevational distribution across a range of elevations. Further along the backbone of the phylogeny, the core Merianieae species range from lowland Atlantic Forest to high Andean elevations (Dellinger et al. 2024). The Davya (Atlantic Forest Merianieae) and *Meriania s. s.* clades of northern Colombia and the Caribbean Antilles are found at lower elevations, while the *Notocentrum* clade has shifted to higher elevations. The Andean Merianieae (including *Notocentrum*) spread to the Brazilian Atlantic Forest, the Greater Antilles and Central America and consist of about 120 species, including the high-elevation genus *Axinaea* (41 described species) with their bulbous connective appendages indicative for the shift to passerine pollination (Michelangeli et al. 2022; Dellinger et al. 2024). Notably, the Andean Merianieae underwent a single colonization event approximately 13.7-10 million years ago (Dellinger et al. 2024). The Adelbertia clade, which includes species from the Guayana Shield (except for the Andean *Meriania urceolata* Triana and Brazilian *Meriania*

calophylla Triana), is a sister clade to both, *Macrocentrum* III and *Adelobotrys*. It ranges from low elevations up to to 2000 m. The *Adelobotrys* clade, which encompasses climbing species and shrubs from the Amazonian and Guayana Shield, including *Meriania subumbellata* Cogn., is found at low elevations (Michelangeli et al. 2022).

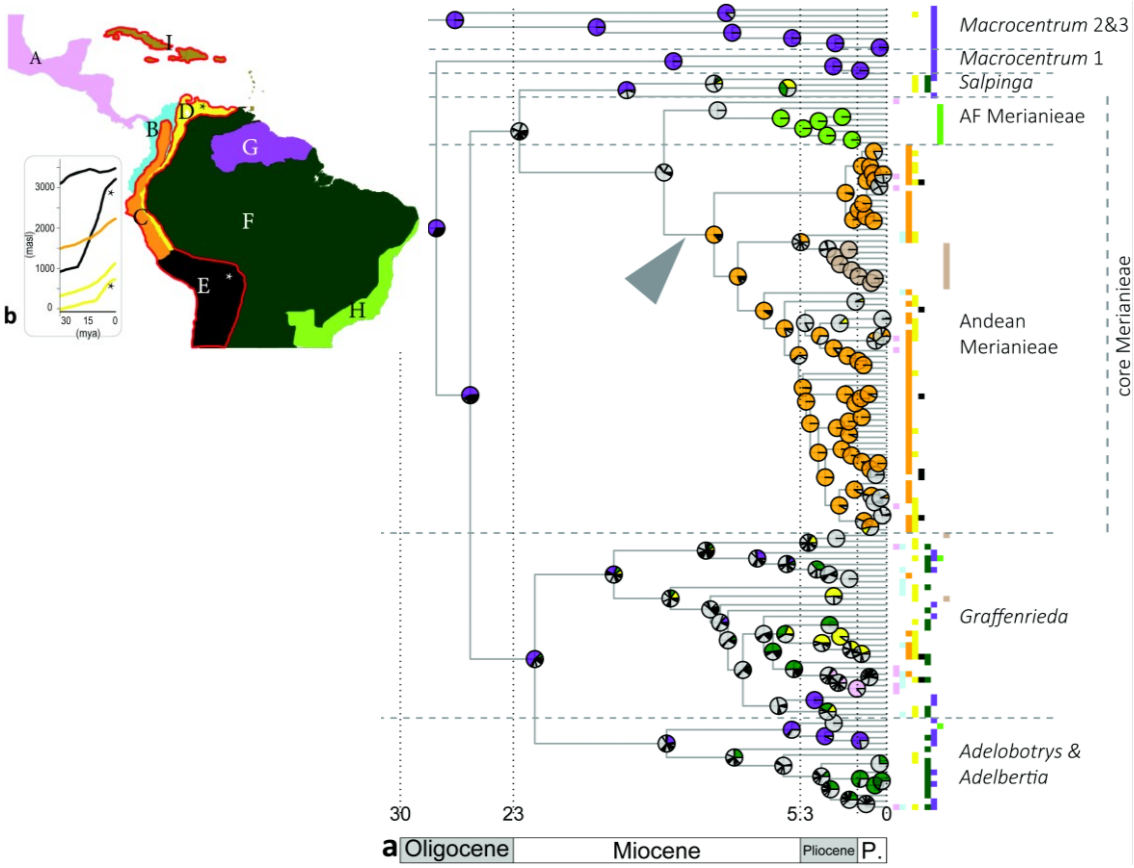

Figure 1 Biogeographic history of Merianieae in the Neotropics: b) Map of the Neotropics showing geomorphological regions: C–E) Andes, F) Amazon Basin, G) Guiana Shield mountains, and H) Atlantic Forest. a) Molecular phylogeny of Merianieae, with an arrow indicating the single colonization event of the Andes that led to increased diversification approximately 13.7–10 million years ago. Modified from Dellinger et al. (2024)

Taxon sampling

To capture a wide morphological and taxonomic diversity within Merianieae, I examined stamens of a total of 69 species (totaling ca. 200 specimens). 132 of these flowers had been collected in the field in Ecuador, Costa Rica, Brazil, Cuba, and Colombia by different researchers, including Agnes Dellinger, Fabián Michelangeli, Darin Penneys, and Frank Almeda, and had been preserved in 70% ethanol. The remaining 57 specimens stem from three herbaria and are dried specimens: the New York Botanical Garden (NYBG), the California Academy of Sciences (CAS), and the Missouri Botanical Garden (MO). I rehydrated these dried specimens (see below) so that they are

comparable to the ethanol-preserved material. I deemed 168 specimens suitable for morphometric analysis, as they were mostly intact. I considered samples appropriate for analysis if the stamen was neither damaged nor shriveled, and if at least three out of five traits could be obtained. Consequently, the present study encompasses 69 species from six of the eight currently recognized genera within the tribe Merianieae, with an elevational range from 85 m to 3200 m.

Rehydration of stamens from herbarium specimens

For rehydration of the 57 stamen samples from herbarium specimens, I submerged the dried flowers/stamens in a solution of 5% NH_4OH + 10% EtOH at 60-70°C for a period of 2-8 hours. This process ensures that the samples regain stainable tissues and regain their original size (Espinosa and Pinedo 2018). I adjusted the time required to the dimensions and thickness of flowers in question to prevent sample dissolution. Subsequently, I washed the samples in FAA to neutralise the ammonium and (deviating from Espinosa and Pinedo (2018)) fixed the samples after 2-4 hours with FAA in a second washing step.

Sample preparation, Critical Point Drying (CPD), mounting

To enhance the soft tissue contrast for micro-CT scanning, I stained all stamen samples (the rehydrated samples and the samples preserved in 70% ethanol) using 1% phototungstic acid (PTA; w/v in 70% EtOH) for a minimum of four days. Next, to reduce the likelihood of movement due to dehydration during the scanning process, I mounted the samples tightly embedded within a cotton-filled modified syringe holder, added a few drops of 70% EtOH at the base of the cotton and the sponge-covered lid (Figure 2a). I then sealed the mounted sample in the syringe holder with parafilm. Prior to scanning, I acclimated the mounted samples for 30 minutes at 35°C to the temperature conditions of the scanning chamber to minimize the movement of cotton due to heat expansion. I applied this method to 117 specimens before I opted to implement critical point drying (CPD) on the remaining 51 samples. CPD has proven to be a superior method for handling fragile specimens as the specimen cavities do not collapse during scanning, which would otherwise result in blurred outcomes. This is particularly true for rehydrated specimens, which are softer than those preserved in EtOH and prone to deformation in cotton embedding. I prepared the samples for CPD by gradual dehydration (1% PTA + 85% EtOH, 20 min; 1% PTA + 96% EtOH, 20 min) before acetone replacement (1% PTA + $(CH_3)_2CO$, 20 min). To prevent contamination of the critical point dryer (Leica Microsystems EM CPD300) from the contrast agent, I washed the samples two times in

acetone. I retrieved stamen from intact flowers depending on size and fragility either before dehydration or after CPD. Prior to scanning, I mounted the dried stamen on metal rods (Figure 2b), using quick-drying translucent nail polish (Essence Cosmetics).

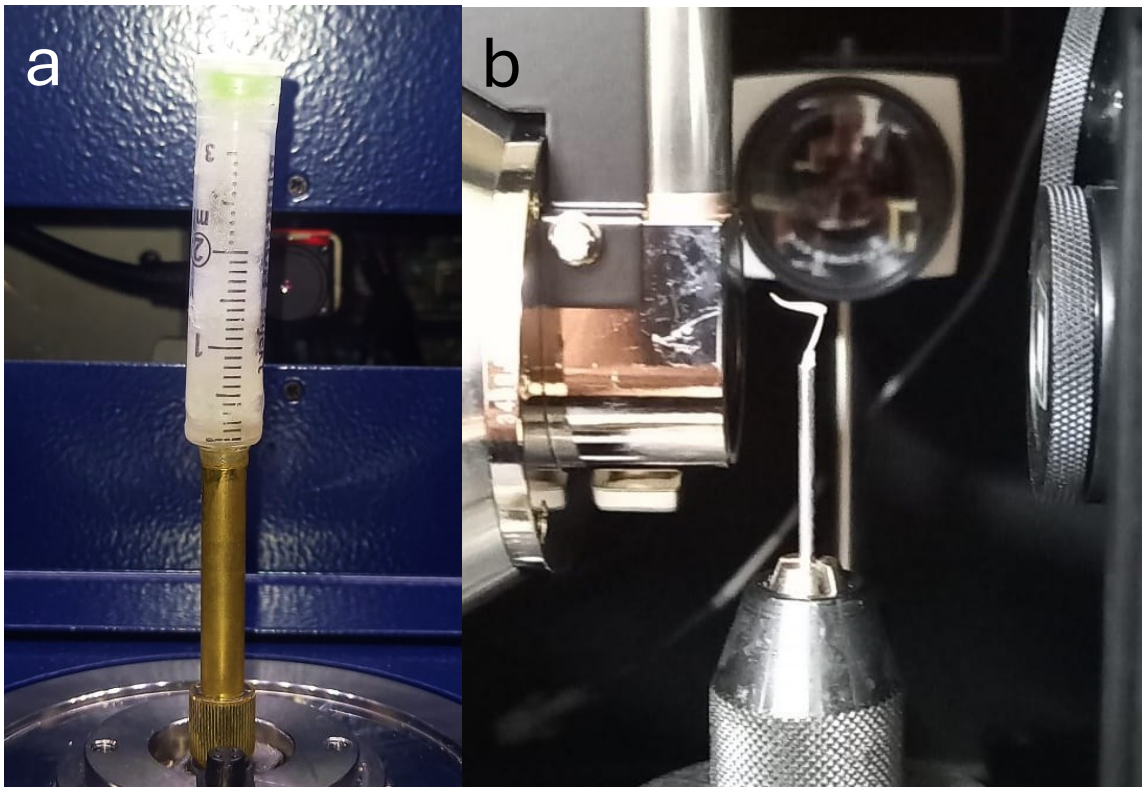

Figure 2 Mounted samples prior to scanning: (a) Sample embedded in a cotton-filled syringe holder with 70% EtOH at the base and a sponge-covered lid in a SkyScan 1275 X-ray Microtomograph system, the stamen itself sits just above the 2 ml mark. (b) Critical point dried (CPD) sample mounted on a metal rod in an Xradia MicroXCT-200 system, the filament was glued to the rod, allowing for perfect reconstruction of the stamen.

X-ray computed tomography and 3D model reconstruction

Depending on size, I performed the 3D scans of specimens on two different computed tomography (ct) scanners:

For specimens of a smaller size (< 6 mm), I employed an Xradia MicroXCT-200 system (Detector: Xradia Inc. in-house; Nikkon optical lense; CCD camera; source: Hamamatsu L9421-02 90 kV Microfocus X-Ray source), which provides scans with very high resolution and is hence suitable for small samples. I conducted the 3D reconstruction of the raw scan data using the software XMReconstructor 8.1.6599 (Xradia Inc.) which produced a picture stack comprising approx. 1200 sections of each sample in DICOM format.

For larger specimens (> 6 mm), I used a SkyScan 1275 X-Ray Microtomograph system (Bruker microCT; tungsten x-ray source, 100 kV, 10 W), which allows for rapid scans of lower resolution, but is perfectly suitable for larger samples. The 3D reconstruction of the raw scan data was conducted using the software NRecon beta 1.7.5.9 (Bruker microCT 2012-19), which generated a picture stack of approx. 1000 sections of each sample in TIF format.

For detailed information regarding the scanning conditions, refer to supplementary material (S 1).

Anther measurements

To capture morphological features of stamens, I visualized the scanned stamens in the imaging programme AMIRA (Version 6.4.0) and measured the following variables: (i) anther length, (ii) appendage volume, (iii) connective volume, (iv) anther pore area, and (v) thecal volume. I defined anther length as the shortest connected distance between the basal end of the thecal lumen and the apical pore (Figure 3a-b). To calculate the pore area, I approximated the pore as an ellipse, and used the maximum diameters (height and width) of the widest opening of the pore [pore_area = π * (height / 2) * (width / 2)] (Figure 3c-d). I obtained the pore and length measurements using the 3D-measurement tool provided in AMIRA (Version 6.4.0). To ensure consistent assessment of appendage volume across samples, I defined the appendage as the dorsal region starting at the point where the filament enters the stamen, clearly distinguishing it from the filamentous structures, connective vascular bundles, and associated tissues. At the apical boundary, I separated the appendage from the connective tissues based on anther type, either at the basal junction of the two thecae or at the point of appendage protrusion in cases where structural differences between the two were not readily apparent (Figure 3e-f). I characterized the connective tissue as the tissue connecting the two thecae, starting from the basal attachment point at the appendage or filament to the apical end (close to the pores). In this study, I use the term ‘thecal volume’ to refer to the internal volume of the theca (lumen) excluding the thecal walls. For the volumes of connectives, appendages and thecae, I used the segmentation editor of AMIRA and delineated the pertinent area in about every 15th 2D-image of the segmented stack of images using the brush tool (Figure 3g). I then exported the interpolated area to a separate material each for connective, appendage and thecal volume (Figure 3h). Subsequently, I obtained the volume using material statistics (Amira XImagePAQ Extension 6.4) for each respective material. I calculated the means of the two thecae and pores, if two were present.

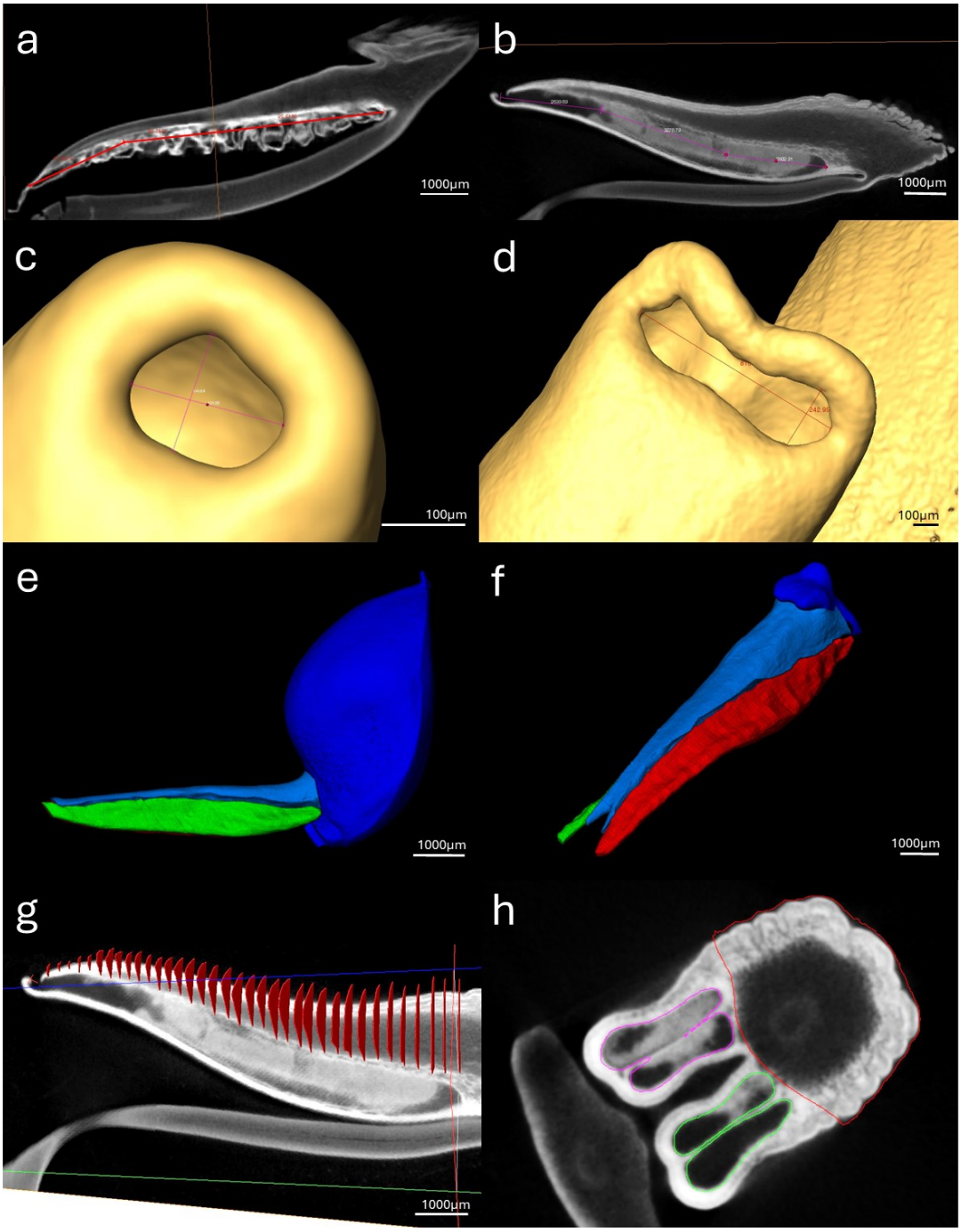

Figure 3 Methodology of anther measurements using AMIRA (Version 6.4.0): a) anther length in Meriania haemantha (Planch. & Linden) Humberto Mend. & Fern.Alonso (bee-pollinated, corrugated thecal walls) b) anther length in Meriania speciosa (Bonpl.) Naudin (bee-pollinated, smooth thecal walls) c) pore size of Axinaea costaricensis Cogn. (passerine-pollianted) d) pore size of M. speciosa (bee-pollinated) e) distinction of materials in A. costaricensis (passerine-pollinated), the appendage is dark blue, the connective light blue and one theca is visible (green) f) distinction of materials in Meriania albiflora Carmenate & Michelang. (NFV-pollinated), with a small appendage (dark blue), prominent connective (light blue), and two thecae (green, red) g) delineation of connective area in approximately every 15th 2D image of the segmented stack of M. speciosa (bee-pollinated), with each brushed area shown as red surface h) 2D view of separated materials in M. speciosa, with outlines of different colors indicating different materials (internal thecal volumes: green, purple; connective: red).

Statistics and reproducibility

I performed all data analyses in R. The phylogenetic tree of the tribe Merianieae and associated information regarding the pollination system and elevational distribution of the species were derived from a cumulative data set of earlier studies by Dellinger et al. (2021b).

I employed the package ‘ggplot2’ (Wickham 2016) for all subsequent bar charts, box plots, and scatter plots in the supplementary materials.

Dataset

Of the 69 species included in the dataset, 39 had 2 to 6 replicates available (S 2). For these species, I calculated average values for each trait. 45 species lacked replicates (due to inadequate specimens) so that the single measurement was included. Further, a total of 34 out of the 69 species included in the dataset are heterantherous, exhibiting either a strong or weak division into feeding and pollinating stamens within a flower (Dellinger et al. 2021b). Of these 34 heterantherous species, I had both stamen types available for only 15 species, and only those 15 were thus amenable to comparative measurements of pollinating and feeding stamens. Consequently, when analysing feeding and pollinating stamens as distinct replicates for heterantherous species, the study includes 84 data points.

Heteranthery

To assess potential patterns between pollinating and feeding stamens, I calculated the ratio of the larger trait value to the smaller trait value for each of the 15 heterantherous species with data available for both anther types and plotted them on a heatmap using the r-package ‘pheatmap’ (Kolde 2019).

Trait differences across pollination systems (phylogenetic ANOVA)

To compare the trait values among pollination systems (pollination system as predictor variable (bee, nectar-foraging-vertebrate, passerine)) while considering the shared ancestry, I performed a phylogenetic ANOVA, using the ‘phylANOVA’ function from the r-packages ‘phytools’ (Revell 2024) and ‘geiger’ (Pennell et al. 2014). The phylogenetic ANOVA corrects for the non-independence of data points due to evolutionary relationships between species. Post-hoc pairwise comparisons were conducted using the Holm method, which adjusts for multiple comparisons in a more general and conservative framework than Tukey’s HSD. I ran the ANOVA on two different data sets,

as a phylogenetic analysis permits only one tip per species, hence both stamen types of heterantherous species could not be represented at the same time, and calculating a mean value of feeding and pollinating stamens would have distorted the results. Therefore, I divided stamens of the heterantherous species into feeding and pollinating stamens. The first data set (het l) includes all values for species with isomorphic stamens and among the heterantherous species, only values for pollinating stamens. The second data set (het s) consists of all values for species with isomorphic stamens and among the heterantherous species, only values for feeding stamens. I ran the two phylogenetic ANOVAs for each of the five traits separately. I used the treedata-function of the package 'phytools' (Revell 2024) to prune the phylogeny to the number of tips matching the number of specimens with available measurements. By removing rows and, consequently, species with missing data due to compromised sample quality, I performed the phylogenetic ANOVAs on datasets with variable sample sizes. The first phylogenetic ANOVA (het l) had the following sample sizes: pore area (53 species), connective volume (69 species), appendage volume (61 species), thecal volume (69 species), and anther length (69 species). The second phylogenetic ANOVA (het s) had the following number of specimens: pore area (44 species), connective volume (52 species), appendage volume (48 species), thecal volume (69 species), and anther length (52 species).

Elevational and phylogenetic influences on anther traits (phylogenetic Linear Regression)

To test for whether elevation has a significant impact on stamen traits while accounting for the non-independence of species due to shared ancestry, I employed phylogenetic linear regressions from the R package 'phylolm' (Ho and Ane 2014). I tested three different models of trait evolution (Brownian Motion, Pagel's Lambda (λ) or an Ornstein-Uhlenbeck (OU)) and compared model fit using the Akaike Information Criterion (AIC). Support for a BM model indicates a random process of trait evolution, support for the Lambda model indicates that the traits are likely to have evolved due to shared ancestry, while support for an OU model indicates that traits have evolved under the influence of selection towards an optimal value. I followed the same protocol as previously described (two data sets (het l, het s), pruning the phylogenetic tree, removing NAs) and employed the phylogenetic linear regression with elevation as the predictor variable for each trait, respectively, for all pollination systems (het l: 69 / het s: 52 species) and on three subsets, bee-pollinated species (het l: 47 / het s: 38 species), nectar-foraging-vertebrate pollinated species (het l: 10 / het s: 10 species), and passerine-pollinated species (het l: 13 / het s: 4 species).

Trait evolution and elevational distribution in different Merianieae clades (phyloContmap)

To visualize the relationships between the elevational distribution of Merianieae and stamen traits, I used barplots for the different trait values and plotted those at the tips of the phylogenetic tree of Merianieae. In addition, I ran ancestral state reconstructions for elevation (continuous trait estimation under maximum likelihood, 'ape' (Paradis and Schliep 2019). I annotated plots to visualize the different lineages within Merianieae following Michelangeli et al. 2022. For heterantherous species, I only included values for feeding stamens (het l).

Phylogenetic Principal Component Analysis (pPCA) of anther traits

Besides assessing how traits evolved independently, I ran joint analyses for all five traits using a phylogenetic PCA. I ran separate phylogenetic PCAs on the full dataset (species representing all pollination systems) and on bee-pollinated species only, to assess more subtle differences among bee-pollinated species. For this purpose, I used the R-packages 'ggplot2' (Wickham 2016), 'ggrepel' (Slowikowski 2024), 'factoextra' (Kassambara and Mundt 2020) and 'gridExtra' (Auguie 2017). By reducing the multidimensionality of the data into the most influential principial components, I was able to explore patterns of morphological variation of specimens with varying pollination systems and within the group of bee-pollinated species, respectively. Regarding heteranthery, I employed the PCA on both complete data sets (het l / het s).

Results

Trait differences across pollination systems – phylogenetic ANOVA

Against my expectations, I could not confirm the hypothesis that vertebrate-pollinated Merianieae generally have larger anther volumes than bee-pollinated Merianieae (Figure 4). The phylogenetic ANOVA demonstrated a statistically significant impact of pollination system on appendage volume only ($F = 27.31$, $p = 0.001$, dataset het l). Pairwise post-hoc comparisons showed that these significant differences stem from passerine-pollinated species having more than ten-fold larger stamen appendages (ca. 13 mm^3) than both the bee-pollinated ($p = 0.003$, ca. 1.5 mm^3) and nectar-foraging-vertebrate-(NFV, ca. 1 mm^3) pollinated ($p = 0.003$) species. The difference between the bee and

NFV groups is not significant and both pollination systems have comparatively small appendage volumes (but note that some bee-pollinated species have appendage volumes in the range of passerine-pollinated volumes).

Second, I could not confirm my hypothesis that vertebrate-pollinated species have larger pores and shorter anthers compared to bee-pollinated species as adaptation to high-quality pollinators (Figure 4). Pore sizes were variable across bee-pollinated species and ranged among the largest values (up to 0.14 mm^2) to the smallest values (< 0.01 mm^2). The average pore area for nectar-foraging-vertebrate-pollinated species was larger, but differences were not significant. Similarly, anther lengths were not different among pollination systems, refuting my hypothesis that shorter anthers (potentially indicative of easier pollen release) correlate with vertebrate pollination. Bee-pollinated species showed the largest range in anther lengths (ca. 1.5-14.5 mm).

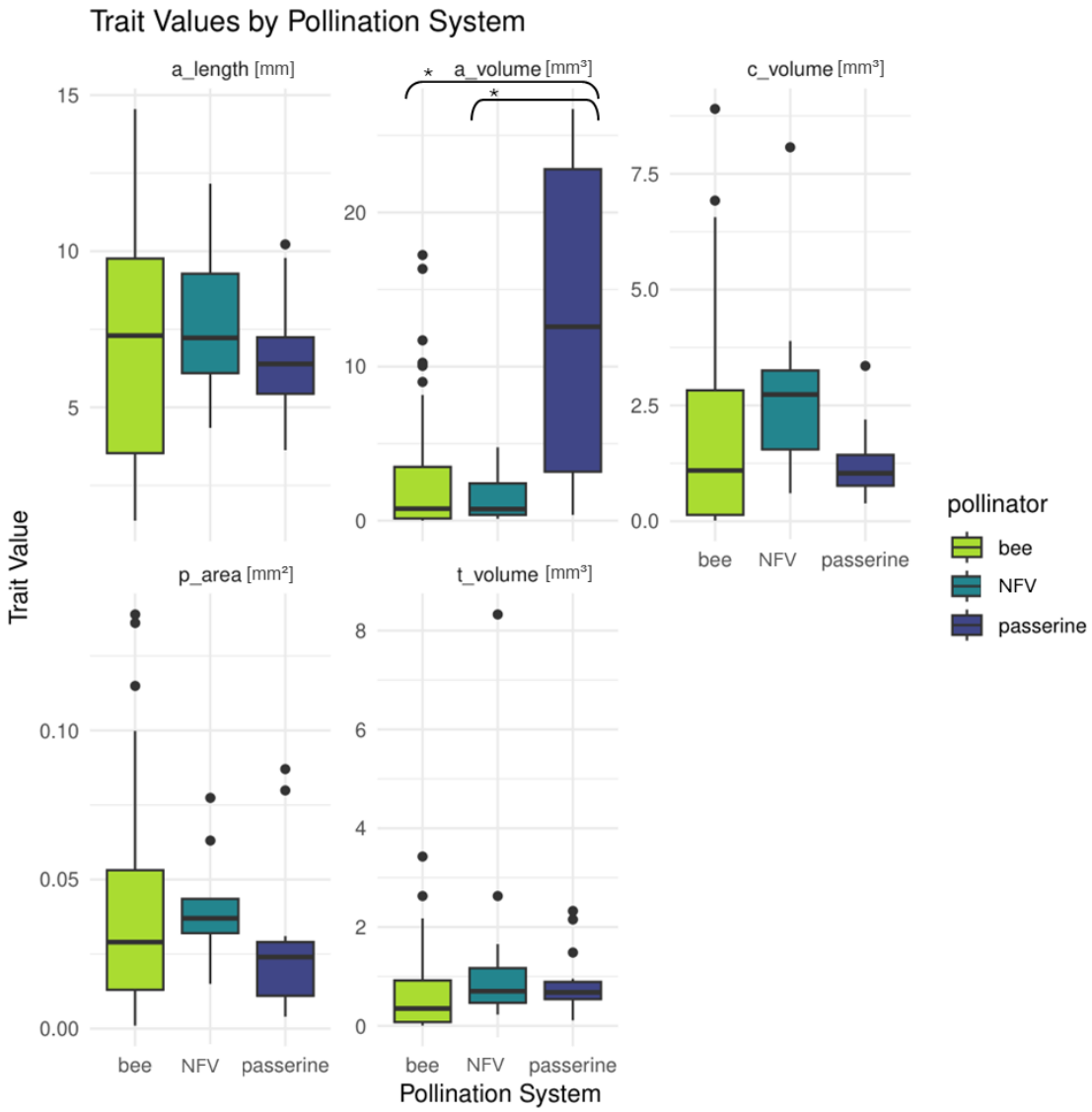

*Figure 4 Boxplots illustrating trait values across pollination systems as visualizations of the phylogenetic ANOVA results. Significant differences (p-values) between pollination systems are denoted by a star above brackets, where * represents p < 0.05.*

Heteranthery

Contrary to my predictions, I could not confirm that heteranthery as a mechanism of refined pollen presentation and dispensing is more prevalent in lowland-bee pollinated Merianieae. Instead, the distribution of heterantherous species along the elevational gradient appears relatively uniform, with no discernible clustering at specific elevations. This pattern holds true for both bee-pollinated species and those which shifted to mixed vertebrate or passerine pollination, which are generally associated with higher elevations (Figure 5). Comparing the 15 species with both stamen types present (S 3), I found that heteranthery can be achieved through size differences in different parts of the stamens. Anther length is the most consistent trait, with stamens classified as “large” always

having longer anthers than stamens classified as “small”. These long-anther stamens tend to have larger connective and thecal volumes. Specifically, 13 out of 15 species show increased connective volumes in pollinating stamens, apart from *Axinaea grandifolia* Triana and *Meriania urceolata*. Additionally, 12 out of 15 species display greater thecal volumes in pollinating stamens, except for *Axinaea alata* E.Cotton, *Meriania maxima* Markgr., and *M. urceolata*. No such trend was recognizable for pore size and appendage volume (note that we could compare appendage volumes only in 13 species). In agreement with these evaluations, a plot of the trait ratios between the two anther types (Figure 6) reveals that the ratio of anther length is relatively consistent across the 15 heterantherous species. Similarly, the ratios for thecal volume and connective volume also exhibit a general consistency but include outlier species with notably high ratios, such as connective volume in *M. urceolata* and thecal volume in *M. calophylla*. No such trend can be seen for appendage volume or pore area.

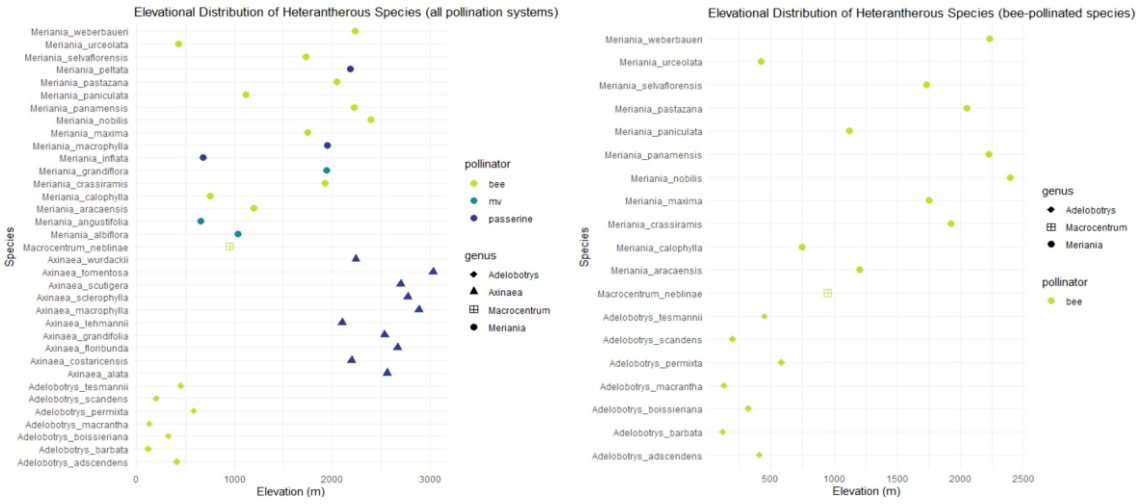

Figure 5 Scatterplot showing the elevational distribution of heterantherous species across pollination systems (left) and bee-pollinated species only (right). Colors represent pollination syndromes, and symbols correspond to genera (see legend for details). Note that species are not ordered by phylogenetic relatedness.

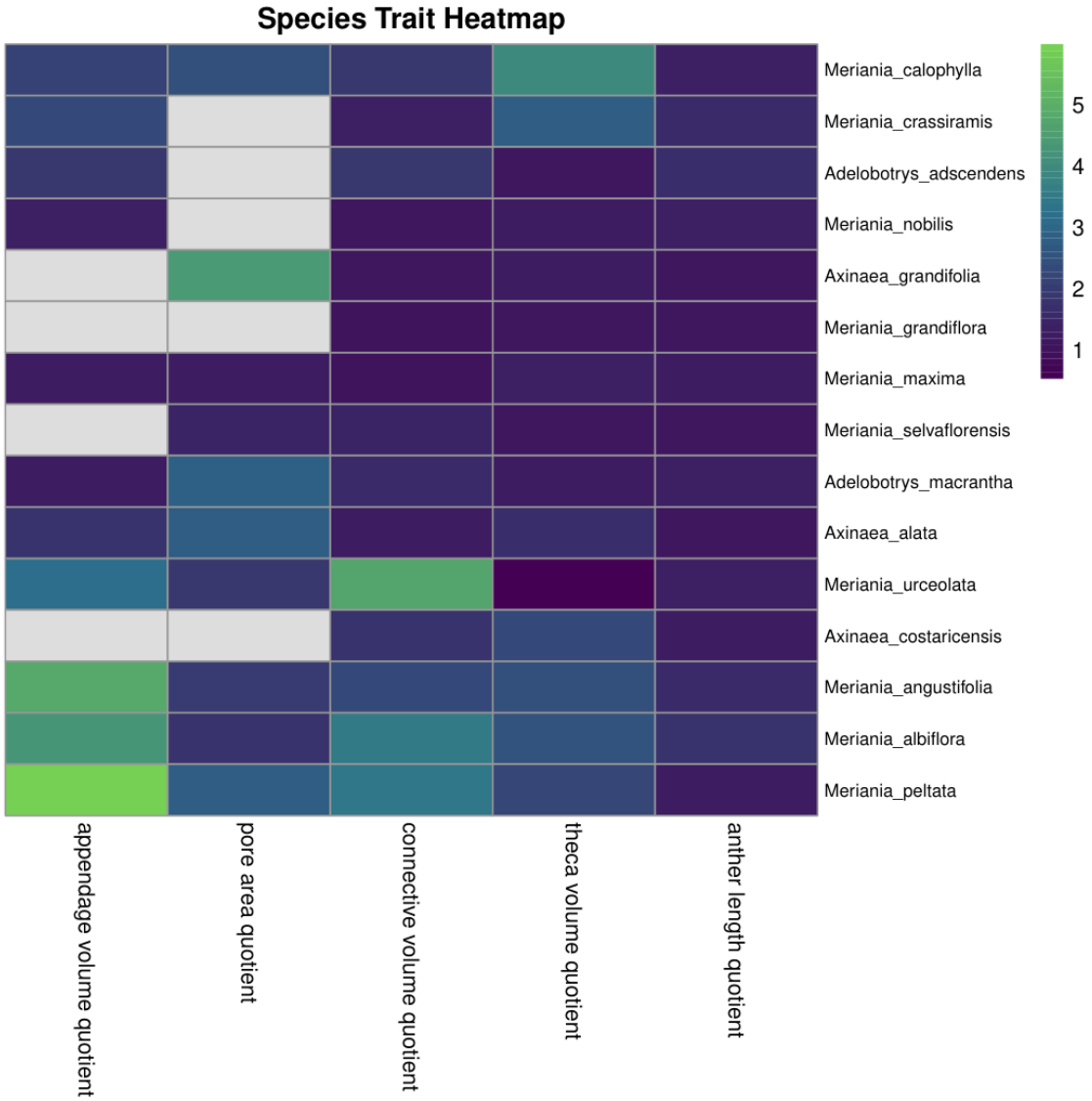

Figure 6 Heatmap illustrating anther trait quotients, representing the ratio of larger to smaller anther trait measurements in heterantherous species. Species are ordered based on hierarchical clustering using the Manhattan distance metric. The color gradient from dark purple to light green indicates low to high quotient values, with missing data shown in grey.

Elevational and phylogenetic influences on anther traits (phylogenetic Linear Regression)

The phylogenetic linear regression on the dataset including pollinating stamens (het I) reveals that appendage volume, pore area and thecal volume significantly increase with elevation across all pollination systems, as well as for the subset of bee-pollinated species (Table 2; for comprehensive results see S 4 and S 5 in the supplementary materials). Across most traits, the Pagel's Lambda (λ) model exhibited a lower Akaike Information Criterion (AIC), suggesting that phylogenetic signal plays a role in explaining

trait variation. However, for appendage volume (across the full dataset and among bee-pollinated species), the Ornstein-Uhlenbeck model (OU, random root) fit the data better, indicating the potential influence of selection (i.e., by pollinators) towards distinct optimal values for this trait. For the dataset of feeding stamens (het s), statistically significant effects are revealed of elevation on connective volume, pore area and thecal volume. I discuss these results in more detail below.

*Table 2 Summary of significant Phylogenetic Linear Regression results. Significance levels (p-values) are denoted by stars, where * represents **p < 0.05**, ** represents **p < 0.01**, and *** represents **p < 0.001**. Marginal effects are indicated by ".", non-significant results "ns". The results are reported for both the Pagel's Lambda (λ) and Ornstein-Uhlenbeck (OUrandomRoot) models.*

Phylogenetic Linear Regression using Pagel's Lambda (λ) and Ornstein Uhlenbeck (OU) model (Elevation)						
	Pollination system	Anther length	Appendage volume	Connective volume	Pore area	Theca volume
Pollinating stamens (het l)	All	ns	*** (OU)	ns	* (λ)	** (λ)
	Bee	ns	** (OU)	ns	* (λ)	* (λ)
	Nectar-foraging-vertebrate	ns	ns	ns	ns	ns
	Passerine	ns	. (λ)	ns	ns	ns
Feeding stamens (het s)	All	ns	ns	* (λ)	* (λ)	** (λ)
	Bee	ns	ns	ns	. (λ)	ns
	Nectar-foraging-vertebrate	ns	. (λ)	ns	ns	ns
	Passerine	. (λ)	. (λ)	ns	ns	. (λ)

All pollination systems

Pollinating stamens (het l)

The phylogenetic linear model (OU) indicates a significant positive impact of elevation on appendage volume across all pollination systems with larger appendage volumes at higher elevations (Estimate = 0.00272466, t = 3.7868, p < 0.001). This model explains 18.7% of the variance in appendage volume (Adjusted R^2 = 0.187) while accounting for the phylogenetic signal (α = 0.3337914). Similarly, applying Pagel's Lambda (λ), elevation has a significantly positive influence on pore area, with pore area increasing

with higher elevations (Estimate = 1.1776e-05, t = 2.4657, $p < 0.05$, Adjusted R^2 = 0.1057, λ = 3.140294e-07). Additionally, a significant positive contribution of elevation was observed on thecal volume, resulting in larger volumes at higher elevations (Estimate = 0.00044575, t = 3.0737, $p < 0.05$, Adjusted R^2 = 0.09261, λ = 1e-07). Among passerine-pollinated species, the appendage volumes trended towards being largest at highest elevations, but this association was not significant (p = 0.07259). No other significant effects of elevation on the remaining traits were found across all pollination systems.

Feeding stamens (het s)

For feeding stamens, the phylogenetic linear model (λ) demonstrates a statistically significant positive impact of elevation on connective volume (Estimate = 0.00079811, t = 2.0607, $p < 0.05$, Adjusted R^2 = 0.05984, λ = 0.1999375), pore area (Estimate = 1.1776e-05, t = 2.4657, $p < 0.05$, Adjusted R^2 = 0.1057, λ = 3.140294e-07), and thecal volume (Estimate = 0.00050758, t = 2.8733, $p < 0.05$, Adjusted R^2 = 0.1246, λ = 1e-07), so that all of these traits are larger at higher elevations. Although no significant effect was found for other traits, appendage volumes tended to be larger with rising elevation in nectar-foraging-vertebrate-pollinated species (p = 0.05623) and larger for three traits in passerine-pollinated species: anther length (p = 0.08529), appendage volume (p = 0.07259), and thecal volume (p = 0.05961). These trends, with traits being greater at higher elevations, although not statistically significant, warrant further investigation with a bigger sample set.

Bee-pollinated Species

Contrary to my expectations, my findings challenge the hypothesis that bee-pollinated species at high elevations exhibit both, larger pores and shorter anthers compared to their lowland counterparts as a result of reduced bee-pollinator availability under harsh environmental conditions. While the phylogenetic linear model results show that pore area increases significantly with elevation, no such relationship was observed for anther length. However, consistent with my predictions, I was able to support the hypothesis that high-elevation bee-buzz-pollinated Merianieae species have larger thecal and appendage volumes in comparison to lowland species. This trend was not, however, observed in connective volume (potentially important for efficient vibration transmission), which showed no significant association with elevation.

Pollinating stamens (het l)

In bee-pollinated species, the phylogenetic linear model (OU) indicates a strong positive impact of elevation on appendage volume, with larger volumes correlated with higher elevations (Estimate = 0.0016306, t = 3.7868, p < 0.01), explaining 14.4% of the variance (Adjusted R^2 = 0.144, α = 0.1210365). Using Pagel's Lambda (λ), a moderate positive influence of elevation was also observed on pore area, tending to be larger at high elevations (Estimate = 1.7290e-05, t = 2.4477, p < 0.05, Adjusted R^2 = 0.128, λ = 0.2547048). A significant positive effect was also detected for thecal volumes, being greater in species at higher elevations (Estimate = 0.00033951, t = 2.3432, p < 0.05, Adjusted R^2 = 0.09261, λ = 0.1781429).

Feeding Stamens (het s)

For feeding stamens in bee-pollinated species, no significant associations with elevation were found. While pore areas tended to be larger at higher elevations, this association was not significant (p = 0.05748), suggesting that also in feeding stamens, pore areas may often be enlarged at higher elevations.

Stamen traits and elevation across Merianieae clades (phyloContmap)

The plotting of trait values as bars adjacent to the phylogeny reveals patterns and trends which might be influenced by both, phylogenetic relationships and adaption to mountain environments. For this analysis, I focused on the dataset including pollinating stamens (het l), as the trait differences were more pronounced. Regarding anther length (Figure 7), it is notable that only the polyphyletic *Macrocentrum* clade and the paraphyletic *Graffenrieda*, irrespective of elevation, are among the shortest anthers when compared to the core Merianieae, Adelbertia and *Adelobotrys* species. However, within this range of species with shorter anthers, *Graffenrieda rotundifolia* (Humb. & Bonpl.) DC. stands out as a lowland outlier, displaying one of the longest anthers. Some but not all species of the Andean *Axinaea* (e.g. *A. grandifolia*, *A. costaricensis* Cogn., *A. sclerophylla* Triana, *A. alata*) exhibit the largest connective appendages (Figure 8), followed by numerous *Meriania* species from the Andean Merianieae. In contrast, lowland clades such as *Macrocentrum* and *Adelobotrys* (apart from *Meriania subumbellata*), as well as Davya and Adelbertia, display smaller appendages. Notably, despite *Graffenrieda* having colonized a wide variety of biogeographic areas, there appears to be no positive relationship between appendage volume and elevation in *Graffenrieda*. The Atlantic Forest Merianieae, as well as the Andean Merianieae, show the largest connective

volumes (Figure 9) as well as a variety of smaller ones. The northern Columbian bee-pollinated species *Meriania speciosa* (Bonpl.) Naudin and *Meriania longifolia* (Naudin) Cogn. of the *Meriania s. s.* clade of mid elevations range among the largest connective volumes, with *M. longifolia* being the largest in this dataset (8.9 mm^3). The two second largest connective volumes occur in *Meriania tomentosa* (Cogn.) Wurdack of the Notocentrum clade and *Meriania sanguinea* Wurdack of the Andean Merianieae. Both species occur at higher elevations and are NFV-pollinated. *Meriania selvaflorensis* Humberto Mend., also of the Andean Merianieae with a large connective volume, on the contrary, is bee-pollinated. In comparison to the aforementioned groups, the *Axinaea* clade exhibits comparatively reduced connective volumes. This is exemplified by species such as *Axinaea scutigera* Triana, which displays lower values than some of the *Adelobotrys* or *Graffenrieda* species. Except *for Graffenrieda rotundifolia*, the *Graffenrieda* and *Macrocentrum* clades exhibit the smallest connective volumes. In terms of pore area (Figure 10), it is evident that the *Macrocentrum* clade exhibits some of the smallest pores. In the core Merianieae, there are the largest pored stamens (*Meriania speciosa*, *Meriania weberbaueri* J.F.Macbr.) as well as some rather short ones. No other discernible trend is apparent, as each clade displays a range of pore sizes, irrespective of elevation. The thecal volume (Figure 11) of Andean Merianieae is notably the largest, although the difference to the smallest volumes of *Macrocentrum*, *Graffenrieda* and *Adelobotrys* is not as pronounced as for other traits. Conspicuously, the thecal volume of *Meriania tomentosa* is more than twice as large as that of the second largest thecal volume (*Meriania longifolia*). However, the linear regression model confirmed the visually observable trend towards increasing thecal volumes with higher elevations. Furthermore, I constructed scatter plots to illustrate the relationship between traits and elevation, which can be found in the supplementary material (S 6 and S 7) for reference.

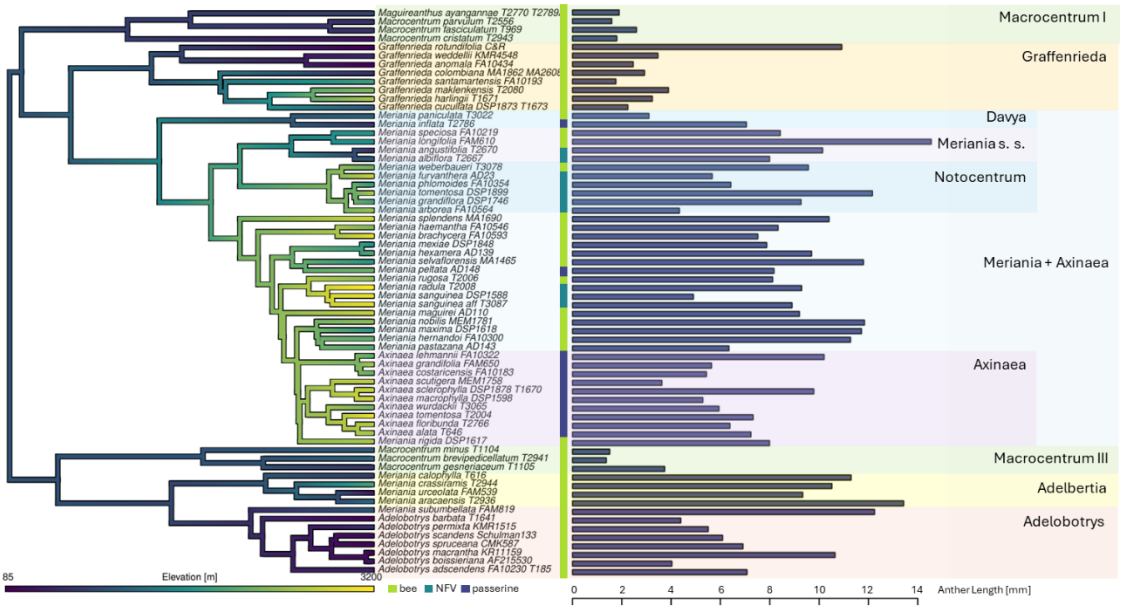

Figure 7 Ancestral character estimation of elevation mapped onto phylogeny of Merianieae with adjacent bar plots representing anther length values for individual species. Elevation is mapped onto the phylogeny, with a color gradient ranging from dark purple (85 m above sea level) to yellow (3200 m above sea level). Pollination syndromes are color-coded (see legend). Distinct Merianieae clades are highlighted in different colors.

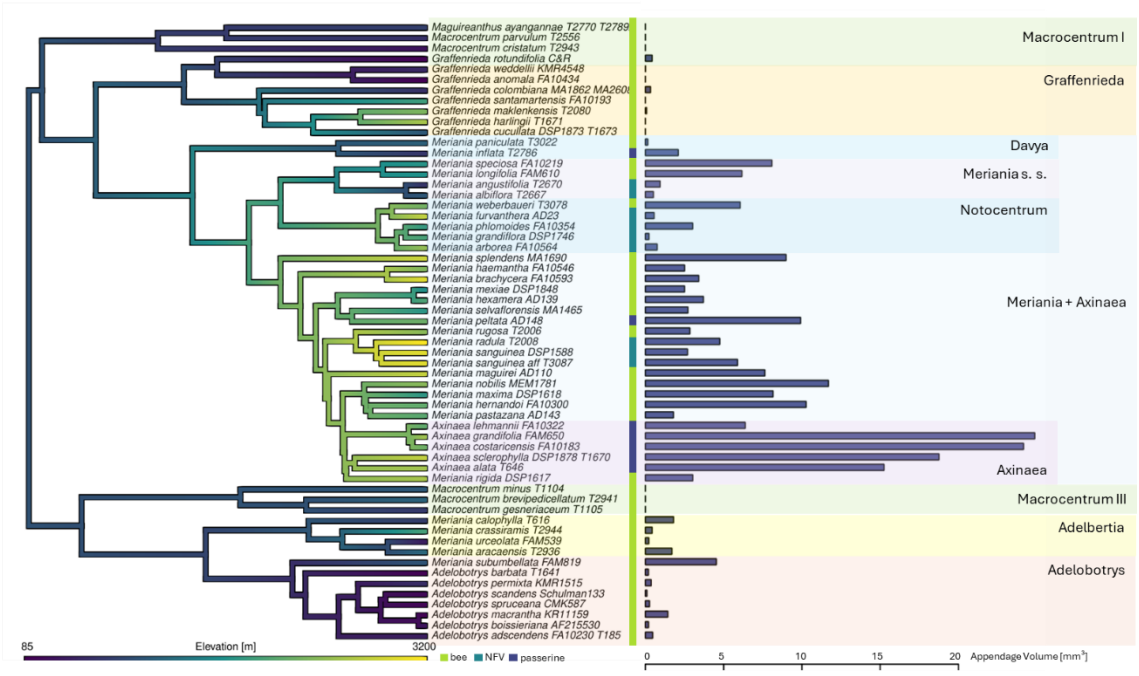

Figure 8 Ancestral character estimation of elevation mapped onto phylogeny of Merianieae with adjacent bar plots representing appendage volume values for individual species. Elevation is mapped onto the phylogeny, with a color gradient ranging from dark purple (85 m above sea level) to yellow (3200 m above sea level). Pollination syndromes are color-coded (see legend). Distinct Merianieae clades are highlighted in different colors.

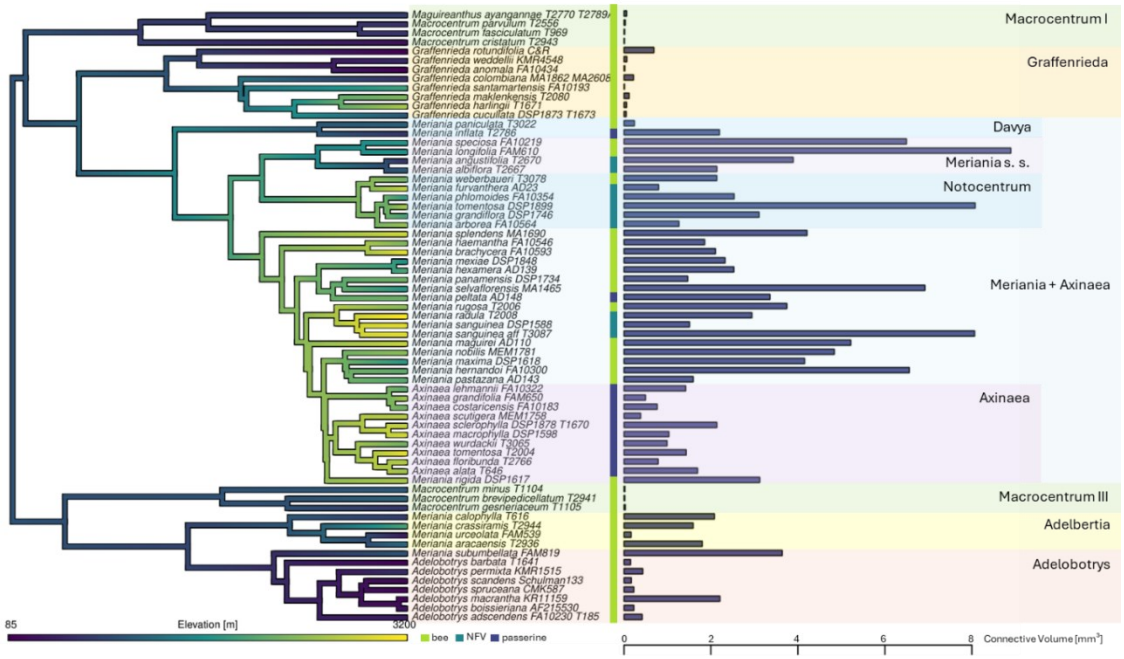

Figure 9 Ancestral character estimation of elevation mapped onto phylogeny of Merianieae with adjacent bar plots representing connective volume values for individual species. Elevation is mapped onto the phylogeny, with a color gradient ranging from dark purple (85 m above sea level) to yellow (3200 m above sea level). Pollination syndromes are color-coded (see legend). Distinct Merianieae clades are highlighted in different colors.

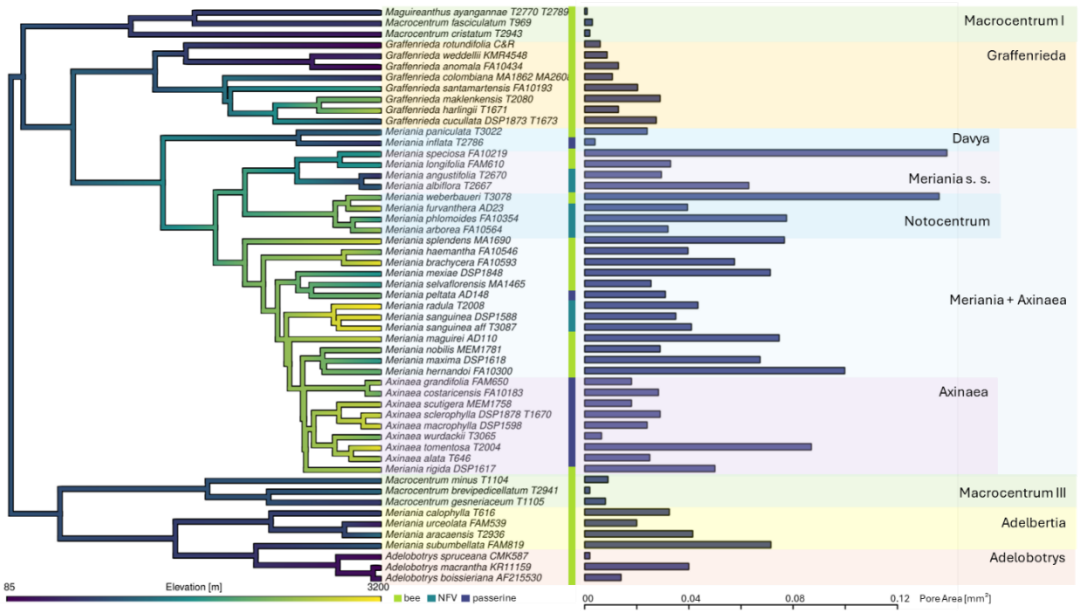

Figure 10 Ancestral character estimation of elevation mapped onto phylogeny of Merianieae with adjacent bar plots representing pore area values for individual species. Elevation is mapped onto the phylogeny, with a color gradient ranging from dark purple (85 m above sea level) to yellow (3200 m above sea level). Pollination syndromes are color-coded (see legend). Distinct Merianieae clades are highlighted in different colors.

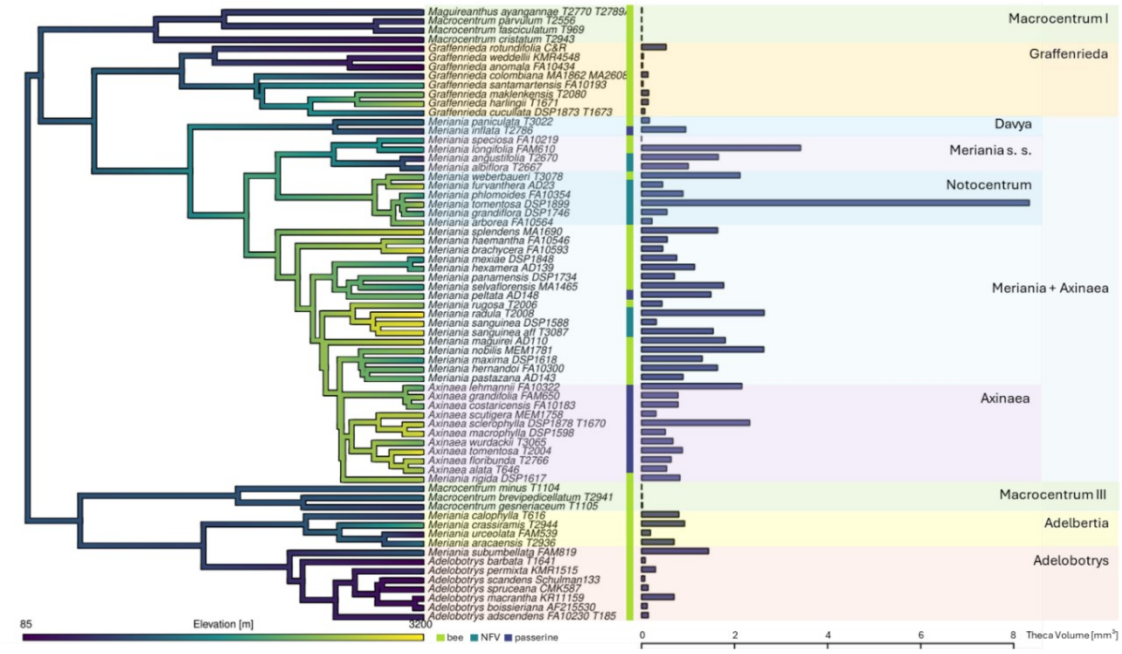

Figure 11 Ancestral character estimation of elevation mapped onto phylogeny of Merianieae with adjacent bar plots representing thecal volume values for individual species. Elevation is mapped onto the phylogeny, with a color gradient ranging from dark purple (85 m above sea level) to yellow (3200 m above sea level). Pollination syndromes are color-coded (see legend). Distinct Merianieae clades are highlighted in different colors.

Phylogenetic Principal Component Analysis (pPCA) of anther traits

All pollination systems

Pollinating stamens (het I)

The phylogenetic PCA of the full dataset (pollinating stamens, het I) reveals that the first two principal components account for 95.17% of the total variance, with PC1 contributing 65.20% and PC2 29.97%. PC1 summarizes variation in appendage volume (loading = -0.9967), while PC2 is strongly influenced by anther length (loading = -0.9596). Connective volume (loading = -0.8256) and thecal volume (loading = 0.7179) play secondary roles in PC2. In contrast, pore area contributes minimally, suggesting it has a negligible influence on species distribution in stamen morphospace. The phylogenetic signal ($\lambda = 0.43$) indicates a moderate phylogenetic structure in the analyzed traits. The corresponding biplot (Figure 12) illustrates clustering of passerine-pollinated species characterized by large appendages along negative PC1, bee-pollinated species from low

elevations with small pores along positive PC2, and mid- to high-elevation *Meriania* species with elongated anthers along negative PC2.

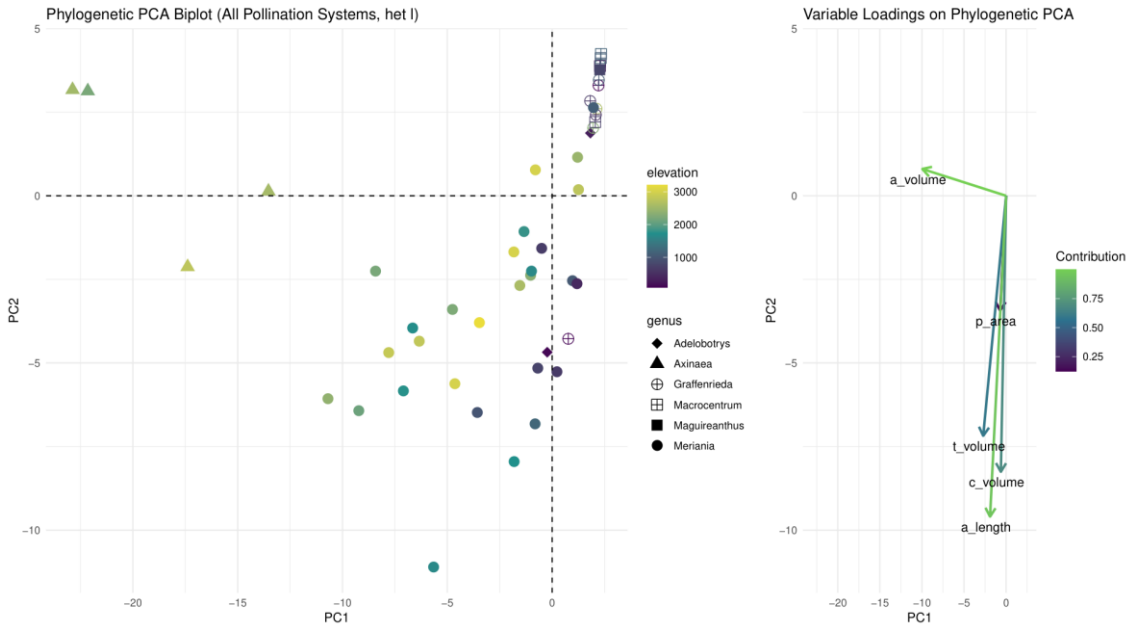

Figure 12 Phylogenetic PCA biplot of the dataset "het l" including pollinating stamens across all pollination systems. Elevation is visualized as a color gradient ranging from dark purple (85 m) to yellow (3200 m). Distinct genera are represented by specific symbols (refer to legend for details). Species are plotted as colored symbols within the morphospace (left panel) based on their principal component scores. The right panel displays the variable loadings, where the direction and length of the vectors indicate the contribution of each trait to the principal components. The color of the vectors (ranging from purple = 0 to light green = 1) further illustrates the relative contribution strength.

Feeding stamens (het s)

Similarly, for feeding stamens (het s), PC1 and PC2 together explain 96.01% of the variance, with a dominant contribution from PC1 (74.06%) and a smaller but substantial contribution from PC2 (21.95%). Again, appendage volume is the primary driver of PC1 (loading = -0.9625), with anther length (loading = -0.6596), connective volume (loading = -0.6390), and thecal volume (loading = -0.6101) also contributing moderately. PC2, on the other hand, is most strongly influenced by anther length (loading = 0.7244) and secondarily by connective volume (loading = 0.6390) and thecal volume (loading = 0.5554). Pore area has a negligible effect, reinforcing its low relevance in explaining variation. The phylogenetic signal (λ = 0.11) suggests weak phylogenetic structuring, highlighting the potential impact of external factors. The biplot (Figure 13) reveals clustering of bee-pollinated species from low elevations with small pores along negative PC2, emphasizing differences in traits across elevation.

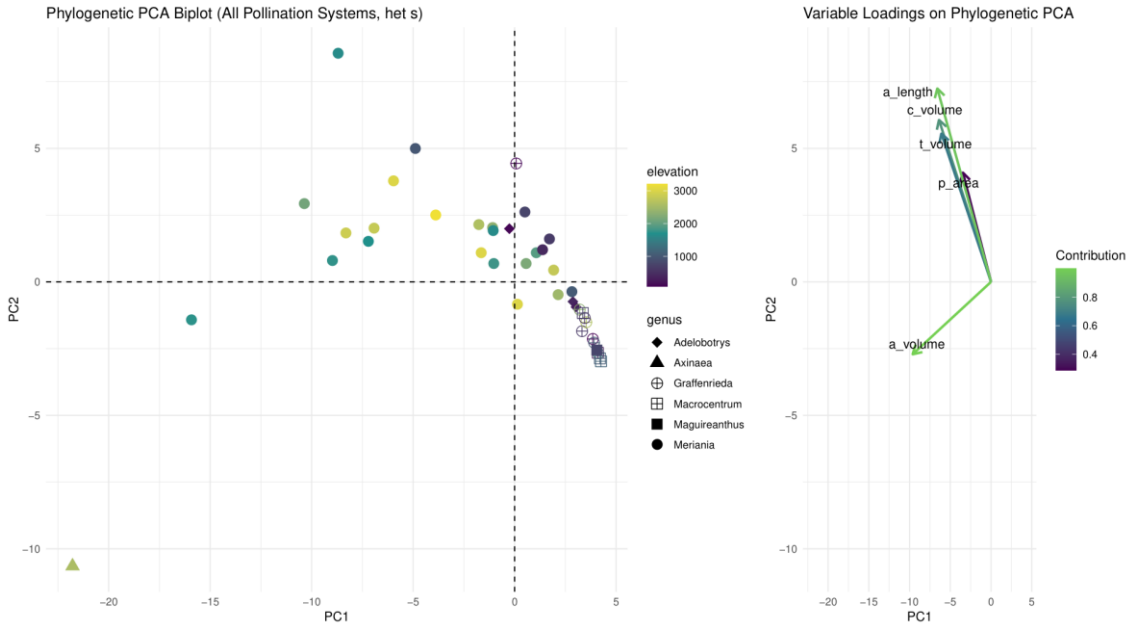

Figure 13 Phylogenetic PCA biplot of the dataset "het s" including feeding stamens across all pollination systems. Elevation is visualized as a color gradient ranging from dark purple (85 m) to yellow (3200 m). Distinct genera are represented by specific symbols (refer to legend for details). Species are plotted as colored symbols within the morphospace (left panel) based on their principal component scores. The right panel displays the variable loadings, where the direction and length of the vectors indicate the contribution of each trait to the principal components. The color of the vectors (ranging from purple = 0 to light green = 1) further illustrates the relative contribution strength.

Bee-pollinated Species

Pollinating stamens (het l)

In the phylogenetic PCA of bee-pollinated species including pollinating stamens (het l) (Figure 14) the first two principal components collectively explain 93.77% of the total variance. PC1, which accounts for 77.28% of the variance, is predominantly driven by anther length (loading = -0.9337), with significant contributions from connective volume (loading = -0.8501), appendage volume (loading = -0.8106), and thecal volume (loading = -0.7854). PC2, contributing 16.49% of the variance, is moderately associated with appendage volume (loading = -0.5719). The phylogenetic signal (λ = 0.37) reflects a moderately low phylogenetic structuring of the traits. The PCA biplot (Figure 14) shows clustering patterns according to elevation and phylogeny, with mid- to high-elevation *Meriania* species characterized by larger appendage volumes along negative PC2, while mid- to low-elevation *Meriania* species with shorter anthers are grouped along positive PC2, and other Merianieae with smaller stamens grouped along positive PC1.

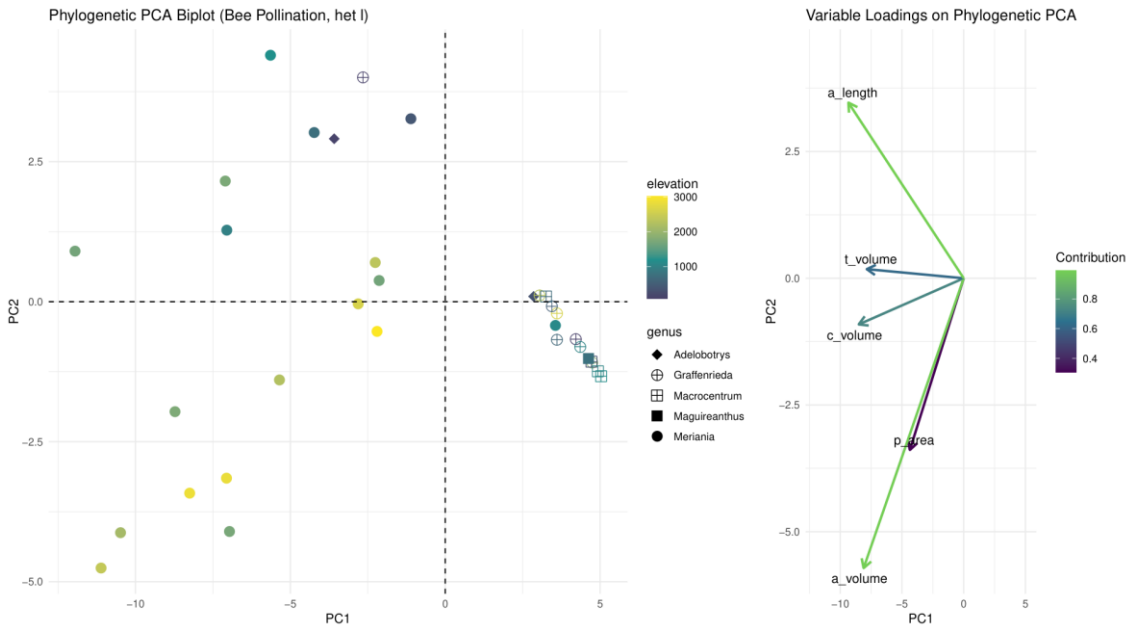

Figure 14 Phylogenetic PCA biplot of the dataset "het l" including pollinating stamens of heterantherous and isomorphic stamens of bee-pollinated species. Elevation is visualized as a color gradient ranging from dark purple (85 m) to yellow (3200 m). Distinct genera are represented by specific symbols (refer to legend for details). Species are plotted as colored symbols within the morphospace (left panel) based on their principal component scores. The right panel displays the variable loadings, where the direction and length of the vectors indicate the contribution of each trait to the principal components. The color of the vectors (ranging from purple = 0 to light green = 1) further illustrates the relative contribution strength.

Feeding stamens (het s)

In the phylogenetic PCA of bee-pollinated species with feeding stamens (het s), PC1 and PC2 explain a combined 95.81% of the total variance. PC1 contributes the majority (79.00%) of the variance and is primarily driven by appendage volume (loading = -0.9079), followed by connective volume (loading = -0.9778), anther length (loading = -0.8739), and thecal volume (loading = -0.7827). PC2, accounting for 16.81% of the variance, is moderately influenced by anther length (loading = -0.4723). The phylogenetic signal (λ = 0.23) suggests a moderate but relatively weak influence of phylogeny on trait variation. The biplot (Figure 15) illustrates scattering of mid- to high-elevation *Merianieae* species with larger appendages along PC2, while mid- to low-elevation species with shorter anthers form a separate cluster at positive PC1.

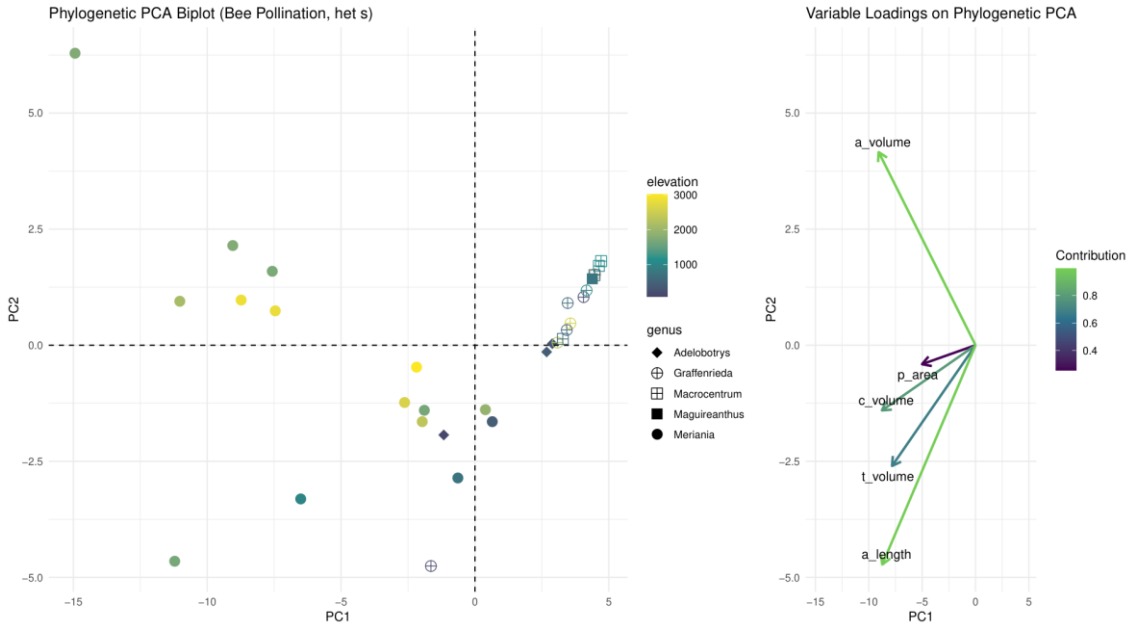

Figure 15 Phylogenetic PCA biplot of the dataset "het s" including feeding stamens of bee-pollinated species. Elevation is visualized as a color gradient ranging from dark purple (85 m) to yellow (3200 m). Distinct genera are represented by specific symbols (refer to legend for details). Species are plotted as colored symbols within the morphospace (left panel) based on their principal component scores. The right panel displays the variable loadings, where the direction and length of the vectors indicate the contribution of each trait to the principal components. The color of the vectors (ranging from purple = 0 to light green = 1) further illustrates the relative contribution strength.

Discussion

Trait differences between pollination systems

Connective, appendage and thecal volume – shift to larger pollinators

> *H1: Nectar-foraging-vertebrate- and passerine-pollinated species of Merianieae exhibit larger connective, appendage, and thecal volumes compared to bee-pollinated species, reflecting the shift to larger pollinators.*

Comparative morphometric analyses of stamen traits in Merianieae, combined with phylogenetic and elevational occurrence data, allowed me to infer changes in stamen morphology across elevations and pollination systems. However, I could not confirm my hypothesis that, reflecting the shift towards larger pollinators, the connective and thecal volumes of NFV- and passerine-pollinated species would be significantly larger than those of bee-pollinated species. Although positive correlations between flower size and

pollinator size with increasing elevation have been reported in other systems (Maad et al. 2013; Delgado et al. 2023), this pattern is not reflected in appendage volumes.

Among my study species, differences in appendage volumes reflect the morphological adaptations required for the mechanisms that facilitate pollen release with different pollination systems. In passerine-pollinated species, connective appendages function as both, a fruitbody reward and a bellows mechanism, ejecting the entire pollen load when compressed by the passerine's beak (Dellinger et al. 2014). Among NFV-pollinated flowers, pollen release is triggered when the vertebrate pollinators touch the soft thecal walls while foraging for nectar, but they do not focus their foraging attention on the appendages (Dellinger et al. 2019a). In bee-pollinated species, however, the dorsal connective appendages are the most diverse in shape from my dataset and range from acuminate and small in *Graffenrieda* to conspicuous and large in *Adelobotrys* and *Meriania* (Dellinger et al. 2019a). These differences in size and shape are likely related to their role during the pollination process, since appendages commonly function as handles to grasp for bees when applying vibrations (Renner 1989). For example, Bochorny et al. (2021) found that the appendages of bee-pollinated flowers, besides serving as handles to grip for buzzing bees, transmit the vibrations produced during buzzing onto the stamens, contributing to a higher pollen release in *Huberia bradeana*.

With that in mind, my results show that the stamens of passerine-pollinated Merianieae species of high Andean elevations are significantly larger in anther connective appendage volume compared to nectar-foraging-vertebrate- (NFV) or buzz-bee-pollinated species. This is consistent with Dellinger et al. (2014), who showed that those species within Merianieae that have shifted to passerine pollination in the Andes of southern Ecuador and northern Peru have enlarged connective appendages that act as a simultaneous bellows organ (to effect pollen expulsion) and food body reward for their pollinators. The mechanism releases the entire pollen load of a single stamen onto the passerine's forehead in a single event (Dellinger et al. 2021a). My data show a marginally significant effect ($p = 0.073$) of elevation on passerine-pollinated species' connective appendages. Given the small sample size of passerine-pollinated species, this result may suggest that appendage volume increases with elevation, even among high-elevation passerine-pollinated species (above 1950 m). Findings by Céspedes et al. (2022), who reported a mid-elevation peak in migrant and resident birds in the Andes, indicate that the abundance of passerine pollinators may decline with elevation. Thus, as pollinator abundance decreases, flowers may compete for limited visits through increased showiness (i.e. larger appendage volumes that pose as fruit body reward). Alternatively, the appendages may simply enlarge in correlation with overall flower size,

which tends to increase with elevation. However, my data show a moderate signal (α= 0.3337914) in the analysis encompassing all pollination systems for the influence of elevation on appendage volume, suggesting that while stabilizing selection plays a role in shaping the trait, shared ancestry moderately exerts a constraint on its evolution. For further studies it would be of interest to link species' elevational occurrence data with pollination observations (frequency of visits, pollinator size), to investigate which factors influence appendage volume among passerine-pollinated species and whether there is an „optimal" appendage volume for maximal pollen release. Similarly, it is unknown how changes in stamen morphology affect pollen release in NFV-pollinated flowers. From what we know, nectar-rewarding Meriania flowers that have shifted to NFV-pollination have more flexible stamens with soft thecal walls that release pollen independent of vibrations via a 'saltshaker' mechanism (Dellinger et al., 2019). The connective appendages of NFV-pollinated species in my dataset are among the smallest in volume, thus I conclude that the pollinators of species that have shifted to the bimodal nectar-foraging-vertebrate syndrome may not exert selective pressure on connective appendages. Experimental assessments may show whether the connective appendages do indeed not play a role in the functionality of the 'saltshaker' mechanism and are a mere remnant from the ancestral state of bee-buzz-pollinated flowers, indicating a loss of function of the appendages.

While my data suggest a non-significant trend toward larger connective volumes in NFV-pollinated species compared to passerine-pollinated species, the evolutionary significance of this pattern remains unclear. Since the NFV-pollinated species of my dataset occur at mid- to high elevations, it is uncertain whether these potentially larger connective volumes represent an adaptation to increased flower size at higher elevations, larger pollinator body size, or a functional contribution to the 'saltshaker' mechanism. This uncertainty aligns with broader patterns of stamen trait variation across elevations. The phylogenetic model encompassing all pollination systems indicates a significant impact of elevation on thecal volume, suggesting that larger thecae at higher elevations may serve as an adaptation to increased pollen production for larger-bodied pollinators.

Pore area and anther length

H2: Nectar-foraging-vertebrate- and passerine-pollinated species of Merianieae have larger pores and shorter anthers compared to bee-pollinated species, driven by higher pollinator efficiency and the shift to nectar and food body rewards at high elevations.

It is widely accepted that flowers frequently visited by pollinators (high pollinator quantity) can maximize reproductive fitness (i.e., high genetic diversity of offspring) by restricting the amount of pollen available per pollinator visit (Percival 1955; Thomson et al. 2000). Such pollen dosing should be particularly strong if pollinators are of "high quality" in the sense that the per-visit pollen transfer rate is high. Bees, which collect pollen to feed their brood, groom themselves and are therefore considered inefficient (i.e., low quality) pollinators. In contrast, passerines foraging for food bodies do not groom and are therefore higher quality pollinators. Pollinators of the NFV syndrome (e.g. rodents, bats, hummingbirds) forage for nectar and lack grooming behavior (Dellinger et al. 2021a), again making them higher quality pollinators. In terms of pollinator quantity, comparatively high pollinator visitation rates have been found in bee-pollinated lowland species, but a significant reduction in bee pollinator visitation rates to Merianieae occurred in mountains (Dellinger et al. 2021b), substantiating my hypothesis that pollen dosing may be relaxed among bee-pollinated species at higher elevations. Among the vertebrate pollinators, hummingbirds visit flowers frequently (Dellinger et al. 2021b), making them high-quantity pollinators, while passerine birds visited flowers infrequently, making them low-quantity pollinators (Table 1). Accordingly, I expected to find highest evidence of floral traits functioning in pollen dosing among lowland bee-pollinated species (high pollinator quantity, low quality) and montane vertebrate-pollinated species (high quality, high quantity). In contrast, I expected low pollen dosing among montane bee-pollinated species (low quantity, low quality) and passerine-pollinated species (low quantity, high quality). With this in mind, the pore size (potentially restricting pollen release) and anther length (shorter anthers signifying shorter travel distances of pollen) of both NFV- and passerine-pollinated species in Merianieae are not significantly larger and shorter, respectively, than those of bee-pollinated species. This finding challenges my hypothesis that an increase in pollinator quality (with the shift to non-pollen collecting pollinators) and the shift to nectar and food body rewards (release from the dual function of pollen as reward and reproductive agent) at high elevations would result in larger pores and shorter anthers. While Brito et al. (2016) found that shifts from small-pored long anthers to large-pored short anthers correlate in the Miconieae tribe of Melastomataceae with shifts from bee-buzz pollinators to generalist pollination (syrphid

flies, wasps), this is not the case for NFV-pollinated Merianieae. My results, although showing a significant positive effect of elevation on pore size, do not support that the increase in pore size is a result of adaptations to more efficient vertebrate pollinators. Nevertheless, the low fit of the model (Adj. $R^2 = 0.1057$, $\lambda = 3.140294e\text{-}07$) shows that pore size is likely shaped by factors other than elevation or phylogeny. While Dellinger et al. (2019) showed that softer thecal walls in NFV-pollinated species allow for easy pollen removal, an additional larger pore size may not be of an evolutionary advantage for the plants. Nevertheless, my results show a non-significant trend towards larger pore size in NFV-pollinated species compared to passerine-pollinated species. However, bee-pollinated species show a wide range of pore sizes, up to three times the size of pores in NFV-pollinated species. Similarly, the median of anther length in passerine-pollinated species is shorter compared to buzz-bee and NFV-pollinated species, yet not significantly so. Overall, it is possible that the complex different pollen release mechanisms found among the three pollination syndromes each require separate optimal adaptations in stamen traits. Investigating in detail how pore size and anther lengths change, i.e., across populations of NFV- or passerine-pollinated species that differ in visitation frequency could give insights on their adaptive value.

Multivariate perspective on stamen morphology

A multivariate perspective allows for a more comprehensive analysis to understand stamen trait functioning, as trait combinations can vary along multiple axes. In the phylogenetic PCA, appendage volume, which significantly influenced the first principal component (PC1), and anther length, which mainly contributed to PC2, drove the morphological variation in stamen traits along two distinct axes. For stamens of passerine-pollinated species, this may indicate that there is an evolutionary constraint for stamens with large appendages to have shorter anthers and vice versa, again indicating that there might be an optimal trait combination for the „bellows“ pollen release mechanism. To investigate this further, I propose for future studies integrating shape analyses of individual stamen traits using geometric morphometrics (landmarks), as commonly applied in the field of anthropology and in some botanical research. Additionally, testing for thecal wall thickness and stiffness, along with assessing the efficiency of pollen transfer to conspecific stigmas in NFV- and passerine-pollinated flowers, may increase our understanding of the factors governing stamen biomechanics in evolutionary shifts away from functionally complex bee-buzz-pollination.

Elevational trait changes among bee-pollinated species

Pore size and anther length – pollinator efficiency

H3: Lowland bee-buzz-pollinated species of Merianieae have smaller pores and longer anthers due to high pollinator quantity but low quality, whereas montane bee-buzz-pollinated species exhibit larger pores and shorter anthers, influenced by reduced pollinator quantity, due to environmental conditions that restrict bee activity and hence select for reduced dispensing mechanisms.

While the data refute my hypothesis that lowland bee-buzz-pollinated species have shorter anthers than montane species, the data confirm that montane bee-buzz-pollinated species have larger pores than lowland species. The moderate to rather low phylogenetic signal of the phylogenetic linear model ($\lambda = 0.2547$) for the influence of elevation on pore size in bee-pollinated species signifies that external factors, rather than phylogeny, contribute to trait variation. As weather conditions become more severe with increasing elevation (lower temperature, more wind, more rain) (Ramos-Jiliberto et al. 2010) and bee-pollinator richness and abundance decreases (Hoiss et al. 2012), flowers benefit from allocating resources to higher quality pollinators (that do not consume pollen, such as vertebrates). Under such reductions of pollination effectiveness of ancestral bee-pollinators, the higher probability of a successful pollination event through more frequent flower visits by vertebrate pollinators may induce evolutionary pollinator shifts (Harder and Thomson 1989; Thomson and Wilson 2008). Alternatively, floral trait changes which maximize pollen transfer even with few bee pollinator visits (i.e., through reduced dispensing mechanisms such as shorter anthers, larger pores) could serve as strategy for coping with low pollinator availability. One group of important cold-adapted bee pollinators are bumblebees, which are capable of generating heat through muscular activity to withstand the harsh environmental conditions at higher elevations (Lawson and Rands 2019). Just like other bees, however, they tend to be inefficient pollinators due to active pollen collection through frequent grooming, resulting in high pollen loss from the plant's perspective. Therefore, bee-pollinated species at high elevations face a dilemma: either allocating a high pollen load (via reduced dispensing) to the few inefficient pollinator visits they may receive throughout the lifespan of a flower (expectation for low pollinator quantity) or distributing small pollen doses among these few pollinators (expectation for low pollinator quality), risking incomplete pollen release and reproductive failure. When monitoring flower visitation rates in tropical mountains, Dellinger et al. (2021b) recorded 1.39 visits per flower per hour for the lowland bee-

pollinated *Adelobotrys adscendens*, while three bee-pollinated Merianieae species above 1885 m had rates of < 0.07 visits per flower per hour and three others were not visited at all during the observation hours. Based on the low pollinator abundance at high elevations, I hypothesize that selection for larger pore size reduces dispensing mechanisms and maximizes pollen delivery across limited bee pollinator visits. Importantly, this macroevolutionary pattern detected by me warrants experimental verification in the future, i.e., by comparing pollen release rates for species with different pore sizes. Since it is often difficult to understand which stamen traits affect pollen release and increases in pore size may often go along with other stamen trait changes, manipulative experiments, i.e., artificially increasing pore size by cutting anther tips, may be required. The difficulty of understanding which traits govern pollen release is reflected in contradictory findings by Kemp and Vallejo-Marín (2021) in *Solanum*. There, the authors found that there is no relationship between pore area and dispensing mechanism, but they also emphasize that the current biophysical model for predicting pollen release (Buchmann and Hurley 1978) may be more accurate for some species than for others. Moreover, as their pollen-release experiments were conducted as greenhouse studies and not in the field, potential relationships of pore size with reduced bee-pollinator availability at high elevations are unknown for *Solanum*. Consequently, it remains unclear whether larger pore sizes in Merianieae facilitate pollen removal and are therefore indicative of reduced dispensing or whether they merely evolved in a correlated manner with increased flower size in adaptation to larger bee pollinators. Hence, besides additional controlled pollination experiments to determine which traits exactly facilitate pollen release, field assessments for different buzz-pollinated lineages, such as *Solanum*, are required to clarify whether reduced pollen dispensing mechanisms generally evolve in environments with reduced bee-pollinator availability.

Returning to my hypothesis, the role of anther length regarding dispensing remains unclear. In theory, long anthers allow for more space for pollen and dispensing, as pollen travels a longer distance to reach the pore. This may be particularly pronounced when anther walls are corrugated and hence additionally restrict the width of anthers, i.e., creating several constrictions throughout the length of the anthers. Although my results do not show a significant effect of elevation on anther length, the relationship is still positive, indicating that anthers are longer at higher elevations. Again, this may be due to a general increase in flower size as an adaptation to larger pollinators at higher elevations.

To incorporate anther length into a biophysical model in a first attempt to calculate the interactions within an anther that ultimately lead to pollen expulsion, Buchmann and

Hurley (1978) modelled the lumen of a buzz pollinated *Solanum* stamen as a tall rectangular box with a small terminal pore, while assuming pollen grains as particles with little pollen kit and hence no clumping. More than 40 years later, Kemp and Vallejo-Marín (2021) calculated the external anther area by measuring anther length and width, and found, that larger (pollinating) stamens released less pollen overall, and at lower pollen release rates. However, their results were not significant for feeding stamens, thus they suggested that species-specific factors not included in their model (e.g. conical anther shape, internal locule structure, pollen grain properties) should be considered in the future. In my research, I examined the relationships between stamen traits, elevation, and pollination systems, to assess whether these traits represent adaptations to pollinator efficiency. However, the role of stamen traits in pollen dispensing has largely been overlooked. One potentially relevant trait in this context is anther wall shape. Kopper et al. (2024), in defining the different pollination syndromes in Melastomataceae, described the "buzz-bee" syndrome as including species with ruminate or smooth thecal walls. With the current biophysical models, it would be interesting to investigate how a corrugated (or ruminant) thecal wall would affect the gradual pollen release, as corrugation could provide obstacles that ultimately lead to more staggered pollen release, compared to smooth thecal walls. To ensure comparability in anther curvature with current methods, I suggest using the ratio of anther length to locule internal surface for future studies. This can be done with the same approach I used for segmenting different stamen tissues based off high resolution X-ray computed tomography scans and using tools such as AMIRA for measurements. Alternatively, it might be possible to re-evaluate the current biophysical model of buzz-pollination using the thecal volume estimates obtained by me, coupling them with actual data on pollen release rates.

Connective, appendage and thecal volume – bee pollinator size

H4: Highland bee-buzz-pollinated species of Merianieae have larger connective, appendage, and thecal volumes than their lowland counterparts, reflecting adaptations to larger montane bee pollinators.

The results show that the stamens of highland bee-buzz-pollinated species of Merianieae are generally larger than their lowland counterparts. This may reflect adaptations to larger montane bee pollinators, as appendage and thecal volume increase significantly with elevation compared to their lowland counterparts. However, I did not find a significant effect of elevation on connective volume in bee-buzz-pollinated species. The low Pagel's lambda ($\lambda = 0.1781429$) of the phylogenetic linear model (λ) of the effect of elevation on thecal volume indicates a moderate to low phylogenetic signal, which shows

that external influences drive the evolution of thecal volume in bee-buzz-pollinated stamen of Merianieae. One such external influence could be the selection for larger stamens (which can also carry higher pollen loads) by larger bee pollinators of high elevations. Lara-Romero et al. (2019) found that body size in hymenopteran pollinators is positively correlated with elevation, whereas small hymenopterans decrease linearly with elevation (Warren et al. 1988). As flower size increases with elevation, this confirms my assumption that the larger stamen size of Merianieae at higher elevations is the evolutionary response to larger bee pollinators.

For appendage volume, the low alpha value ($\alpha = 0.1210365$) of the phylogenetic model (OU random root) for the influence of elevation on appendage volume in bee-pollinated species challenges the assumption that larger appendages are an adaptation towards an evolutionary optimum. A high alpha value would indicate a stronger “pull” towards a distinct evolutionary optimum (i.e., an optimal appendage volume), which is not supported here. Overall, however, since the OU model fit the appendage volume data best, the gradual increase in appendage volume may be adaptive with high elevation bees. Again, the exact function of large stamen appendages in pollen release in buzz-pollinated flowers remains to be determined experimentally (i.e., compare Bochorny et al. 2021).

Multivariate perspective on stamen morphology

The multivariate analysis of bee-pollinated species reveals distinct areas of stamen trait space occupied. *Meriania* species at intermediate elevations occupy a separate morphospace from those at lower and higher elevations. This distinction is primarily driven by opposing loadings of anther length and appendage volume along PC2, suggesting that bee-pollinated *Meriania* species either have large appendages and shorter anthers (with larger pores) or smaller appendages and longer anthers (with smaller pores). This division along PC2 supports expectations from pollen presentation theory (Table 1), as montane *Meriania* species (inhabiting environments with fewer, low-quality bee pollinators) predominantly exhibit traits associated with reduced pollen dosing (i.e., large appendages, shorter anthers, larger pores). Furthermore, the multivariate analysis shows that species from other genera (*Adelobotrys, Macrocentrum, Graffenrieda, Maguireanthus*) typically exhibit diminutive stamens and occupy a distinct morphospace, suggesting that stamen trait evolution may have played a less significant adaptive role in these groups.

Biogeographic phylogenetic patterns of trait variation

Considering biogeographic phylogenetic relationships, patterns of trait variation become apparent. As the Andes were colonized by the genus *Meriania* in a single event, the mountain adapted bee-pollinated flowers share a single evolutionary origin (Dellinger et al. 2024). Mapping stamen traits and pollination syndromes onto a phylogeny (Figure 7-11) reveals similar trait expression among core Merianieae that have colonized the Andean mountains, particularly in appendage volume, connective volume, pore size and thecal volume. (Notably, the passerine-pollinated *Axinaea* exhibit the largest appendage volumes). This aligns with the results of the phylogenetic model, which indicate a significant influence of elevation on appendage volume, pore size and thecal volume. No significant effect of elevation was detected for connective volume. However, lowland Guiana shield species from *Macrocentrum* I and III exhibit similarly low trait values to *Adelobotrys* (which extends to the Amazonian Basin), forming a distinct cluster in the morphospace and differing primarily in anther length. *Adelobotrys* displays shorter anthers than *Macrocentrum* I and III, as well as most *Graffenrieda* species from my data set. This contradicts my thesis that long anthers indicate dispensing mechanisms and are more prevalent in lowland bee-pollinated species, which are visited frequently by inefficient pollinators. Contrary to predictions, the genus *Graffenrieda*, which spans a widespread elevational gradient (Dellinger et al. 2024), shows surprisingly little trait variation with elevation. Solely pore area appears to increase with higher elevations in *Graffenrieda* species (Figure 10), indicating that larger pores may confer some benefits, whether by reducing dispensing for less frequent bee pollinators, accommodating larger bee pollinators at higher elevations, or responding to other external factors. Considering the wide elevational range across diverse climatic niches and its largely conserved traits, the genus *Graffenrieda* presents an ideal system for testing subtle trait variation in pore size along elevation gradients. Testing species of different elevations using artificial buzzing experiments combined with pollination observations in the field, could provide valuable insights into the role of pore size in pollen dispensing schedules in Melastomataceae.

Heteranthery

H5: Heteranthery, as a mechanism of refined pollen placement and dispensing, is more prevalent in lowland-bee pollinated Merianieae (where bees are more common) and reflected through morphological diversity in connective, appendage or thecal volumes.

In theory, heteranthery evolves when more pollen is removed by pollinators than is beneficial to the plant (Vallejo-Marín et al. 2009). To counteract this waste of resources, the plant deposits pollen on body parts that are harder for bees to groom, while still attracting pollinators with pollen that is easy to gather (Vallejo-Marín et al. 2009). However, I did not find support in my data for my hypothesis that heteranthery as a mechanism of refined pollen placement and dispensing is more prevalent in lowland bee-pollinated Merianieae, where bees are more common. I found that morphological differentiation of dimorphic stamens can be achieved through size differentiation of different stamen parts, specifically anther length, connective volume or thecal volume: Long-anther stamens tend to have larger connective and thecal volumes. Whilst I expected these traits to be positively correlated, as these differences between feeding and pollinating stamens are often also visible to the eye, I did not expect to find inconsistent results for appendage volume. Nevertheless, Trevizan et al. (2023) found that the overall anther length was longer in pollinating stamens within the stamen of Melastomataceae. Although this is consistent with my results, their study did not include connective and appendage volumes. The enlarged appendage volumes of dimorphic stamens in passerine-pollinated Merianieae have evolved as both a food-body reward and a bellows mechanism (Dellinger et al. 2014). Before the shift to passerine pollination (Dellinger et al. 2021a), the dimorphic ancestral stamens of bee-pollinated species likely evolved according to the “division of labour” hypothesis (Darwin 1899), where feeding stamens attract pollinators, and pollinating stamens facilitate pollen transfer (H. Müller 1881, 1882; F. Müller 1883; Trevizan et al. 2023).

While the „division of labour“ hypothesis is commonly accepted as functional explanation for the evolution of heteranthery, empirical support of the hypothesis is mixed (Kay et al. 2020). Telles et al. (2020) found in *Pterolepis glomerata* (Rottb.) Miq. (Melastomataceae) that feeding stamens and pollinating anther appendages were indistinguishable to bees, yet bees preferred unmanipulated flowers with both anther sets present. This suggests that pollinating anther appendages play a role in attracting pollinators, even though bees have learned that the smaller feeding stamens contain more pollen for this species. However, in *Microlicia cordata* (Spreng.) Cham. (Melastomataceae), Velloso et al. (2018) described a clear distinction in size, color and pollen quantity between pollinating and

feeding stamens: pollinating stamens were larger, produced more pollen and were pink (less visually attractive to bees), whereas feeding stamens were smaller, produced less pollen (but of the same viability as pollinating stamens), were yellow (more visually attractive to bees), and were located more centrally in the flower. Surprisingly, neither study fully supported the 'division of labour' hypothesis, except for the spatial arrangement of the two stamen whorls in the flower, which should, theoretically, allow pollinating stamens to place pollen on areas of the bee's body that are harder to groom, and therefore more successful in reaching the stigmas of conspecific flowers.

Conclusion and future perspectives

In this study, I demonstrate that the comparative morphometric approach using computed tomography (CT) scans to calculate and measure stamen traits using the imaging software AMIRA (version: 4.6.0 NVIDIA 442.50) can indeed be used to draw conclusions on morphological differences in stamen traits between pollination systems and dimorphic stamens within Merianieae. I found that the bulbous connective appendages of passerine-pollinated species of high Andean elevations are significantly larger than those of bee- and NFV-pollinated species, reflecting the shift to fruit body rewards and bellow's pollen release in passerine-pollinated Merianieae. Furthermore, my data suggest that with the bellows' mechanism, there may be an evolutionary or biomechanical trade-off on anther length and appendage volume: As appendage volume increases, anther length decreases.

Although not significant, species which shifted to nectar rewards and pollination by mixed assemblages of vertebrate pollinators show a trend towards larger connective volumes compared to passerine- and bee-pollinated species. With a larger sample size of NFV-pollinated species, comparative statements about the stamen trait combination that constitutes the 'saltshaker' mechanism may be within reach.

My data show that the appendage volume, pore size and thecal volume increase significantly with elevation in buzz-bee-pollinated species. The rather low phylogenetic signal for these traits, as indicated by the phylogenetic models (S 4 and S 5), suggests that external factors rather than phylogeny are responsible for these changes. Assuming that, according to the Pollen Presentation Theory (PPT), flowers frequently visited by low-quality pollinators enhance their reproductive success by limiting pollen release per visitor (Percival 1955; Thomson et al. 2000) and that pollinator quantity decreases with elevation (Warren et al. 1988), the need for reduced dispensing to maximize pollinator effectiveness may be reflected in the morphological changes observed at high

elevations. While the enlargement in anther traits could also be an adaptation to larger-sized montane bee pollinators (Lara-Romero et al. 2019), the role of adaptive trait changes toward reduced dispensing in maximizing pollinator efficiency should not be overlooked. However, for further studies, I suggest performing pollen release experiments across species with contrasting trait extremes (i.e. short vs. long anthers, small vs. large appendage volume, smooth vs. corrugated thecal walls, etc.) to improve our understanding of the factors governing pollen release and their impact on pollinator efficiency and dispensing mechanisms. Additionally, quantifying other stamen traits responsible for dispensing within Merianieae (e.g. thecal wall shape, thickness, and stiffness) in addition to volumetric measurements such as performed in this study may further refine current biophysical models of pollen expulsion. Despite the remaining gaps, the comparative morphometric approach presented here represents the first detailed quantification of internal stamen volumes of buzz-pollinated flowers and serves as a foundation for further analyses to determine which traits influence pollen release. Based on the current data, the comparative morphometric approach proves to be powerful for quantifying the differences in dimorphic stamens within heterantherous species. These morphological differences, which are somewhat visible to the naked eye, have historically been challenging to quantify. By assessing anther length, appendage volume, connective volume, pore size and thecal volume, I found that pollinating stamens consistently exhibit larger dimensions in anther length, connective volume and thecal volume. Especially when coupled with experimental assessments, I believe that this refined approach for stamen trait measurements may allow for the more detailed determination of stamen trait functioning during buzz-pollination, and biomechanical changes in flowers associated with shifts away from buzz-pollination.

Acknowledgements

I express my profound gratitude to Agnes Dellinger, for her guidance, expertise, and constructive feedback throughout this project, as well as for her evaluation and comments. I would also like to express my gratitude to my colleagues and members of the Plant-Animal Interactions (PAIn) Laboratory, namely Benjamin Lazarus, Konstantin Kopper, Johan Urrea Cardenas, Viktoria Chiara Wieser, and Andrea Errante. Their discussions, feedback, and support, both academically and emotionally, were most helpful. I would like to express my appreciation for the methodological assistance provided by Susanne Pamperl, Margarita Lachmayer, and Andrea Frosch-Radivo, whose expertise greatly contributed to this research. The University of Vienna, particularly the Department of Botany and Biodiversity Research, Division of Structural and Functional

Botany, is acknowledged for offering an academic environment and the resources necessary to complete this study. Ursula Schachner and the administrative staff are thanked for their logistical support. Finally, I express my gratitude to my sister Sabrina Polz for always being there, my mother Maria Polz-Schlögl, my father Reinhold Polz and my grandmothers Theresia Schlögl and Johanna Polz for their encouragement and practical support. I want to express my gratitude to Tom Eicher, Linus Nwokeke, Lucie Slapakova, Valentina Rigger, and Isabelle Kurz, for their love and friendship. Special thanks to my therapist Ingrid Lawatsch, whose guidance has helped me to find the structure I needed to complete this work. Finally, I want to thank the Waacking Vienna community for growing together in dance training and for providing a safe(er) space.

Text editing adjustments

I edited the raw text of single paragraphs and sentences with DeepL write and OpenAI Chat-GPT 2024 using the following prompt: “Refine for scientific writing style, improve clarity and conciseness, suggest synonyms, but keep my writing style”. I checked the results and applied some of the changes.

References

Bartkowska, Magdalena P., and Mark O. Johnston. 2012. “Pollinators Cause Stronger Selection than Herbivores on Floral Traits in *Lobelia Cardinalis* (Lobeliaceae).” *New Phytologist* 193 (4): 1039–48. https://doi.org/10.1111/j.1469-8137.2011.04013.x.

Bochorny, T., L. F. Bacci, A. S. Dellinger, F. A. Michelangeli, R. Goldenberg, and V. L.G. Brito. 2021. “Connective Appendages in Huberia Bradeana (Melastomataceae) Affect Pollen Release during Buzz Pollination.” *Plant Biology* 23 (4): 556–63. https://doi.org/10.1111/plb.13244.

Brito, Vinícius L.G., and Marlies Sazima. 2012. “Tibouchina Pulchra (Melastomataceae): Reproductive Biology of a Tree Species at Two Sites of an Elevational Gradient in the Atlantic Rainforest in Brazil.” *Plant Systematics and Evolution* 298 (7): 1271–79. https://doi.org/10.1007/s00606-012-0633-5.

Brito, Vinícius L. G., T. G. Fendrich, E. C. Smidt, I. G. Varassin, and R. Goldenberg. 2016. “Shifts from Specialised to Generalised Pollination Systems in Miconieae (Melastomataceae) and Their Relation with Anther Morphology and Seed Number.” *Plant Biology* 18 (4): 585–93. https://doi.org/10.1111/plb.12432.

Buchmann, S. L., and J. P. Hurley. 1978. “Biophysical Model for Buzz Pollination in Angiosperms.” *Journal of Theoretical Biology* 72: 639–57.

Buchmann, S. L. 1983. “Buzz Pollination in Angiosperms.” In *Handbook of Experimental Pollination Biology*, edited by C. E. Jones and R. J. Little, 73–113. New York: Van Nostrand Reinhold Co.

Castellanos, Maria Clara, Paul Wilson, Sarah J Keller, Andrea D Wolfe, and James D Thomson. 2006. “Anther Evolution: Pollen Presentation Strategies Pollinators Differ.” *The American Naturalist V*ol. 167 (2): 288-96

Céspedes Arias, Laura N., Scott Wilson, and Nicholas J. Bayly. 2022. “Community Modeling Reveals the Importance of Elevation and Land Cover in Shaping Migratory Bird Abundance in the Andes.” *Ecological Applications* 32 (1). https://doi.org/10.1002/eap.2481.

Darwin, Francis. 1899. “The Botanical Work of Darwin.” *Annals of Botany* 13: ix–xix.

Delgado, Tamiris, Laura Carolina Leal, Juliana Hanna Leite El Ottra, Vinicius Lourenço Garcia Brito, and Anselmo Nogueira. 2023. “Flower Size Affects Bee Species Visitation Pattern on Flowers with Poricidal Anthers across Pollination Studies.” *Flora* 299 (February). https://doi.org/10.1016/j.flora.2022.152198.

De Luca, Paul A., and Mario Vallejo-Marín. 2013. “What’s the ‘Buzz’ About? The Ecology and Evolutionary Significance of Buzz-Pollination.” *Current Opinion in Plant Biology* 16 (4): 429–35. https://doi.org/10.1016/j.pbi.2013.05.002.

Dellinger, Agnes S., Darin S. Penneys, Yannick M. Staedler, Lena Fragner, Wolfram Weckwerth, and Jürg Schönenberger. 2014. “A Specialized Bird Pollination System with a Bellows Mechanism for Pollen Transfer and Staminal Food Body Rewards.” *Current Biology* 24 (14): 1615–19. https://doi.org/10.1016/j.cub.2014.05.056.

Dellinger, Agnes S., Marion Chartier, Diana Fernández-Fernández, Darin S. Penneys, Marcela Alvear, Frank Almeda, Fabián A. Michelangeli, Yannick Staedler, W. Scott Armbruster, and Jürg Schönenberger. 2019a. “Beyond Buzz-Pollination – Departures from an Adaptive Plateau Lead to New Pollination Syndromes.” *New Phytologist* 221 (2): 1136–49. https://doi.org/10.1111/nph.15468.

Dellinger, Agnes, Léa Pöllabauer, Milan Loreti, Janis Czurda, and Jürg Schönenberger. 2019b. "Testing Functional Hypotheses on Poricidal Anther Dehiscence and Heteranthery in Buzz-Pollinated Flowers." *Acta ZooBot* 156: 197–214. Accessed March 4, 2025. https://www.researchgate.net/publication/337911167.

Dellinger, Agnes Sophie, Silvia Artuso, Diana Margoth Fernández-Fernández, and Jürg Schönenberger. 2021a. “Stamen Dimorphism in Bird-Pollinated Flowers: Investigating Alternative Hypotheses on the Evolution of Heteranthery.” *Evolution* 75 (10): 2589–99. https://doi.org/10.1111/evo.14260.

Dellinger, Agnes S., Rocio Pérez-Barrales, Fabián A. Michelangeli, Darin S. Penneys, Diana M. Fernández-Fernández, and Jürg Schönenberger. 2021b. “Low Bee Visitation Rates Explain Pollinator Shifts to Vertebrates in Tropical Mountains.” *New Phytologist* 231 (2): 864–77. https://doi.org/10.1111/nph.17390.

Dellinger, Agnes S., Ashley M. Hamilton, Carolyn A. Wessinger, and Stacey D. Smith. 2023. “Opposing Patterns of Altitude-Driven Pollinator Turnover in the Tropical and Temperate Americas.” *The American Naturalist* 202 (2): 152–65. https://doi.org/10.1086/725017.

Dellinger, Agnes S., Laura Lagomarsino, Fabián Michelangeli, Stefan Dullinger, and Stacey D. Smith. 2024. “The Sequential Direct and Indirect Effects of Mountain Uplift, Climatic Niche, and Floral Trait Evolution on Diversification Dynamics in an Andean Plant Clade.” *Systematic Biology* 73 (3): 594–612. https://doi.org/10.1093/sysbio/syae011.

Espinosa, Felipe, and Myreya Pinedo Castro. 2018. “On The Use of Herbarium Specimens for Morphological and Anatomical Research.” *Botany Letters* 165 (3–4): 361–67. https://doi.org/10.1080/23818107.2018.1451775.

Harder, Lawrence. D., and James. D. Thomson. 1989. “Evolutionary Options for Maximizing Pollen Dispersal of Animal- Pollinated Plants.” *The American Naturalist* 133 (3): 323–44. https://doi.org/10.1086/284922.

Hoiss, Bernhard, Jochen Krauss, Simon G. Potts, Stuart Roberts, and Ingolf Steffan-Dewenter. 2012. “Altitude Acts as an Environmental Filter on Phylogenetic Composition, Traits and Diversity in Bee Communities.” *Proceedings of the Royal Society B: Biological Sciences* 279 (1746): 4447–56. https://doi.org/10.1098/rspb.2012.1581.

Ivey, Christopher T., Pocholo Martinez, and Robert Wyatt. 2003. “Variation in Pollinator Effectiveness in Swamp Milkweed, Asclepias Incarnata (Apocynaceae).” *American Journal of Botany* 90 (2): 214–25. https://doi.org/10.3732/ajb.90.2.214.

Kay, Kathleen M., Tania Jogesh, Diana Tataru, and Sami Akiba. 2020. “Darwin’s Vexing Contrivance: A New Hypothesis for Why Some Flowers Have Two Kinds of Anther: Heteranthery in Clarkia.” *Proceedings of the Royal Society B: Biological Sciences* 287 (1941). https://doi.org/10.1098/rspb.2020.2593.

Kemp, Jurene E., and Mario Vallejo-Marín. 2021. “Pollen Dispensing Schedules in Buzz-Pollinated Plants: Experimental Comparison of Species with Contrasting Floral Morphologies.” *American Journal of Botany* 108 (6): 993–1005. https://doi.org/10.1002/ajb2.1680.

Kopper, Constantin, Jürg Schönenberger, and Agnes S. Dellinger. 2024. “High floral disparity without pollinator shifts in buzz-bee-pollinated Melastomataceae.” *New Phytologist* 242 (5): 2322–37. https://doi.org/10.1111/nph.19735.

Lara-Romero, Carlos, Jaume Seguí, Antonio Pérez-Delgado, Manuel Nogales, and Anna Traveset. 2019. “Beta Diversity and Specialization in Plant–Pollinator

Networks along an Elevational Gradient." *Journal of Biogeography* 46 (7): 1598–1610. https://doi.org/10.1111/jbi.13615.

Lawson, David A., and Sean A. Rands. 2019. "The Effects of Rainfall on Plant–Pollinator Interactions." *Arthropod-Plant Interactions* 13 (4): 561-69. https://doi.org/10.1007/s11829-019-09686-z.

LeBuhn, Gretchen, and Kent Holsinger. 1998. "A Sensitivity Analysis of Pollen-Dispensing Schedules." *Evolutionary Ecology* 12: 111–21.

Maad, Johanne, W. Scott Armbruster, and Charles B. Fenster. 2013. "Floral Size Variation in Campanula Rotundifolia (Campanulaceae) along Altitudinal Gradients: Patterns and Possible Selective Mechanisms." *Nordic Journal of Botany* 31 (3): 361–71. https://doi.org/10.1111/j.1756-1051.2013.01766.x.

Michelangeli, F. A., A. S. Dellinger, R. Goldenberg, F. Almeda, H. Mendoza-Cifuentes, D. M. Fernández-Fernández, C. Ulloa Ulloa, and D. S. Penneys. 2022. "Phylogenetics and Taxonomy of Merianieae." In *Systematics, Evolution and Ecology of Melastomataceae*, edited by R. Goldenberg, F. Almeda, and F. A. Michelangeli, 255–73. Cham, Switzerland: Springer.

Mitchell, Randall J., William G. Wilson, Karsten G. Holmquist, and Jeffrey D. Karron. 2013. "Influence of Pollen Transport Dynamics on Sire Profiles and Multiple Paternity in Flowering Plants." *PLoS ONE* 8 (10): e76312. https://doi.org/10.1371/journal.pone.0076312.

Müller, F. 1883. Two kinds of stamens with different functions in the same flower. Nature 27:364-365.

Müller, H. 1881. Two kinds of stamens with different functions in the same flower. Nature 24:307-308.

Müller, H. 1882. Two kinds of stamens with different functions in the same flower. Nature 26:30.

Ne'Eman, Gidi, Andreas Jürgens, Linda Newstrom-Lloyd, Simon G. Potts, and Amots Dafni. 2010. "A Framework for Comparing Pollinator Performance: Effectiveness and Efficiency." *Biological Reviews* 85 (3): 435–51. https://doi.org/10.1111/j.1469-185X.2009.00108.x.

Oliveira, Larissa C., Alberto L. Teixido, Renata Trevizan, and Vinícius L. G. Brito. 2020. "Bee-Mediated Selection Favors Floral Sex Specialization in a Heterantherous

Species: Strategies to Solve the Pollen Dilemma." *Plants* 9 (12): 1685. https://doi.org/10.3390/plants9121685.

Penneys, Darin S., Frank Almeda, Marcelo Reginato, Fabián A. Michelangeli, Renato Goldenberg, Peter W. Fritsch, and R. Douglas Stone. 2022. "A New Melastomataceae Classification Informed by Molecular Phylogenetics and Morphology." In *Springer eBooks*, 109–65. https://doi.org/10.1007/978-3-030-99742-7_5.

Percival, M. S. 1955. "The Presentation of Pollen in Certain Angiosperms and Its Collection by *Apis mellifera*." *New Phytologist* 54 (3): 353–68. https://doi.org/10.1111/j.1469-8137.1955.tb06192.x.

Ramos-Jiliberto, Rodrigo, Daniela Domínguez, Claudia Espinoza, Gioconda López, Fernanda S. Valdovinos, Ramiro O. Bustamante, and Rodrigo Medel. 2010. "Topological Change of Andean Plant-Pollinator Networks along an Altitudinal Gradient." *Ecological Complexity* 7 (1): 86–90. https://doi.org/10.1016/j.ecocom.2009.06.001.

Renner, Susanne S. 1989. "A Survey of Reproductive Biology in Neotropical Melastomataceae and Memecylaceae." *Annals of the Missouri Botanical Garden* 76: 496–518. https://doi.org/10.2307/2399497.

Stebbins, G. L. 1970. "Adaptive Radiation of Reproductive Characteristics in Angiosperms, I: Pollination Mechanisms." *Annual Review of Ecology, Evolution, and Systematics* 1: 307–326.

Telles, Francismeire Jane, Cristian Luan Klunk, Fabiano Rodrigo Maia, Vinícius de Lourenço Garcia Brito, and Isabela Galarda Varassin. 2020. "Towards a New Understanding of the Division of Labour in Heterantherous Flowers: The Case of *Pterolepis glomerata* (Melastomataceae)." *Biological Journal of the Linnean Society* 131 (1): 1–12. https://doi.org/10.1093/biolinnean/blaa081.

Thomson, James D., Paul Wilson, Michael Valenzuela, and Maria Malzone. 2000. "Pollen Presentation and Pollination Syndromes, with Special Reference to Penstemon." *Plant Species Biology* 15 (1): 11–29. https://doi.org/10.1046/j.1442-1984.2000.00026.x.

Thomson, James D., and Paul Wilson. 2008. "Explaining Evolutionary Shifts Between Bee and Hummingbird Pollination: Convergence, Divergence, and Directionality."

International Journal of Plant Sciences 169 (1): 23–38. https://doi.org/10.1086/523361.

Trevizan, Renata, Ana Paula Souza Caetano, Vinicius L. G. Brito, Paulo Eugênio Oliveira, and Francismeire Jane Telles. 2023. “Stamen and Pollen Heteromorphism Linked to the Division of Labour in Melastomataceae Species.” *Flora* 305 (May): 152315. https://doi.org/10.1016/j.flora.2023.152315.

Vallejo-Marín, Mario, J. S. Manson, J. D. Thomson, and S. C.H. Barrett. 2009. “Division of Labour within Flowers: Heteranthery, a Floral Strategy to Reconcile Contrasting Pollen Fates.” *Journal of Evolutionary Biology* 22 (4): 828–39. https://doi.org/10.1111/j.1420-9101.2009.01693.x.

Vallejo-Marín, Mario. 2019. “Buzz Pollination: Studying Bee Vibrations on Flowers.” *New Phytologist* 224 (3):1068-74. https://doi.org/10.1111/nph.15666.

Velloso, Mariana de Souza Carvalho, Vinícius Lourenço Garcia de Brito, Ana Paula Souza Caetano, and Rosana Romero. 2018. “Anther Specializations Related to the Division of Labor in Microlicia Cordata (Spreng.) Cham. (Melastomataceae).” *Acta Botanica Brasilica* 32 (3): 349–58. https://doi.org/10.1590/0102-33062017abb0358.

Warren, S. D., K. T. Harper, and G. M. Booth. 1988. “Elevational Distribution of Insect Pollinators.” *The American Midland Naturalist* 120 (2): 325–30. https://doi.org/10.2307/2426004.

Xiao, Chang Long, Hui Deng, Gan Ju Xiang, Kadiori Edwin Luguba, You Hao Guo, and Chun Feng Yang. 2017. “Sequential Stamen Maturation and Movement in a Protandrous Herb: Mechanisms Increasing Pollination Efficiency and Reducing Sexual Interference.” *AoB PLANTS* 9 (3). https://doi.org/10.1093/aobpla/plx019.

R-packages

Auguie, Baptiste. 2017. “gridExtra: Miscellaneous Functions for "Grid" Graphics.” R package version 2.3. https://CRAN.R-project.org/package=gridExtra.

Ho, L. S. T., and C. Ane. 2014. "A Linear-Time Algorithm for Gaussian and Non-Gaussian Trait Evolution Models." Systematic Biology 63 (3): 397–408.

Kassambara, Alboukadel, and Fabian Mundt. 2020. “factoextra: Extract and Visualize the Results of Multivariate Data Analyses.” R package version 1.0.7. https://CRAN.R-project.org/package=factoextra.

Kolde, Raivo. 2019. “pheatmap: Pretty Heatmaps.” R package version 1.0.12. https://CRAN.R-project.org/package=pheatmap.

Paradis, Emmanuel, and Klaus Schliep. 2019. "ape 5.0: An Environment for Modern Phylogenetics and Evolutionary Analyses in R." Bioinformatics 35: 526–28. https://doi.org/10.1093/bioinformatics/bty633.

Pennell, Matthew W., Joseph M. Eastman, G. J. Slater, J. W. Brown, J. C. Uyeda, R. G. FitzJohn, Michael E. Alfaro, and Luke J. Harmon. 2014. "geiger v2.0: An Expanded Suite of Methods for Fitting Macroevolutionary Models to Phylogenetic Trees." Bioinformatics 30: 2216–18.

Revell, Liam J. 2024. "phytools 2.0: An Updated R Ecosystem for Phylogenetic Comparative Methods (and Other Things)." PeerJ 12: e16505.

Slowikowski, Kamil. 2024. “ggrepel: Automatically Position Non-Overlapping Text Labels with 'ggplot2'.” R package version 0.9.5. https://CRAN.R-project.org/package=ggrepel.

Wickham, Hadley. 2016. “ggplot2: Elegant Graphics for Data Analysis.” Springer-Verlag New York.

Supplementary materials

S 1 Overview of scanning setting parameters for all specimens

Scan-ID	Method	Species	Scanner	Camera binning	Acceleration voltage [kV]	Source current [uA]	Pixel size [um]	Optical magnification	Exposure time [s]	Pictures per sample
AD7	EtOH	*Meriania hernandoi*	SkyScan	1.000	50.000	200.000	10.000	1.000	0.035	901.000
CT_078	EtOH	*Axinaea macrophylla*	SkyScan	1.000	40.000	175.000	7.000	1.000	0.100	1029.000
CT_079	CPD	*Meriania macrophylla*	Micro-CT	1.000	30.000	200.000	7.100	1.000	3.000	1200.000
CT_080a	CPD	*Meriania mexiae*	SkyScan	1.000	35.000	175.000	7.000	1.000	0.085	1029.000
CT_084_neu	EtOH	*Meriania maguirei*	SkyScan	1.000	35.000	175.000	7.000	1.000	0.050	1029.000
CT_085b	CPD	*Axinaea lehmannii*	SkyScan	1.000	40.000	175.000	7.000	1.000	0.100	1029.000
CT_090	CPD	*Meriania maxima*	SkyScan	1.000	40.000	180.000	8.000	1.000	0.072	1029.000
CT_092	CPD	*Meriania haemantha*	SkyScan	1.000	40.000	175.000	7.500	1.000	0.080	901.000
CT_094	EtOH	*Meriania splendens*	SkyScan	1.000	40.000	175.000	10.000	1.000	0.050	1029.000
CT_096_l	EtOH	*Meriania selvaflorensis*	SkyScan	1.000	35.000	175.000	7.000	1.000	0.050	1029.000
CT_097	CPD	*Meriania hernandoi*	SkyScan	1.000	40.000	175.000	7.000	1.000	0.100	901.000
CT_099	EtOH	*Meriania phlomoides*	SkyScan	1.000	35.000	175.000	7.000	1.000	0.050	1029.000
CT_100	EtOH	*Meriania phlomoides*	SkyScan	1.000	35.000	175.000	7.000	1.000	0.050	1029.000
CT_101	CPD	*Meriania phlomoides*	Micro-CT	1.000	30.000	200.000	8.130	1.000	3.000	1200.000
CT_102	CPD	*Meriania phlomoides*	SkyScan	1.000	40.000	175.000	8.000	1.000	0.080	901.000
CT_103	CPD	*Meriania phlomoides*	SkyScan	1.000	40.000	175.000	8.000	1.000	0.080	901.000
CT_104	CPD	*Meriania phlomoides*	SkyScan	1.000	40.000	150.000	7.000	1.000	0.100	1029.000
CT_105	CPD	*Meriania maguirei*	SkyScan	1.000	40.000	175.000	7.500	1.000	0.060	1029.000
CT_106	CPD	*Meriania radula*	SkyScan	1.000	40.000	150.000	7.000	1.000	0.100	901.000
CT_107	EtOH	*Axinaea costaricensis*	SkyScan	1.000	40.000	175.000	7.000	1.000	0.050	1029.000
CT_108	CPD	*Axinaea costaricensis*	SkyScan	1.000	40.000	175.000	7.000	1.000	0.080	1029.000
CT_109	EtOH	*Axinaea costaricensis*	SkyScan	1.000	40.000	175.000	7.000	1.000	0.050	1029.000

CT_110	CPD	*Axinaea costaricensis*	SkyScan	1.000	35.000	175.000	7.000	1.000	0.085	1029.000
CT_111	CPD	*Graffenrieda weddellii*	Micro-CT	1.000	25.000	200.000	2.020	4.000	3.000	1200.000
CT_112	CPD	*Axinaea grandifolia*	SkyScan	1.000	40.000	175.000	7.000	1.000	0.080	1029.000
CT_113	CPD	*Graffenrieda cucullata*	Micro-CT	1.000	25.000	200.000	1.450	4.000	5.000	1200.000
CT_114_b	CPD	*Meriania mexiae*	SkyScan	1.000	35.000	175.000	7.000	1.000	0.080	1029.000
CT_115	CPD	*Graffenrieda colombiana*	Micro-CT	1.000	25.000	200.000	1.600	4.000	2.000	1200.000
CT_116	CPD	*Graffenrieda anomala*	Micro-CT	1.000	30.000	200.000	2.020	4.000	4.000	1200.000
CT_117	CPD	*Meriania arborea*	Micro-CT	1.000	30.000	200.000	2.700	4.000	4.000	1200.000
CT_118	EtOH	*Meriania brachycera*	SkyScan	1.000	40.000	175.000	7.000	1.000	0.050	1029.000
CT_119	CPD	*Graffenrieda santamartensis*	Micro-CT	1.000	30.000	200.000	0.960	4.000	3.000	1200.000
CT_120	EtOH	*Graffenrieda maklenkensis*	SkyScan	1.000	40.000	175.000	7.000	1.000	0.050	1029.000
CT_127	CPD	*Adelobotrys adscendens*	Micro-CT	1.000	25.000	200.000	4.880	1.000	4.000	1200.000
CT_128	CPD	*Adelobotrys adscendens*	Micro-CT	1.000	30.000	200.000	4.200	1.000	4.000	1200.000
CT_130	CPD	*Adelobotrys adscendens*	Micro-CT	1.000	30.000	200.000	4.200	1.000	4.000	1200.000
CT_142	CPD	*Axinaea sclerophylla*	SkyScan	1.000	40.000	175.000	8.500	1.000	0.080	901.000
CT_146_a	CPD	*Meriania urceolata*	Micro-CT	1.000	25.000	200.000	6.420	1.000	4.000	1200.000
CT_146_b	CPD	*Meriania urceolata*	Micro-CT	1.000	30.000	200.000	9.220	1.000	3.000	1200.000
CT_148	CPD	*Meriania inflata*	Micro-CT	1.000	40.000	200.000	8.130	1.000	2.000	1200.000
CT_150	EtOH	*Axinaea alata*	SkyScan	1.000	40.000	175.000	7.000	1.000	0.050	1029.000
CT_150b	CPD	*Axinaea alata*	SkyScan	1.000	40.000	175.000	7.000	1.000	0.080	901.000
CT_151_a	CPD	*Meriania albiflora*	Micro-CT	1.000	25.000	200.000	8.470	1.000	4.000	1200.000
CT_151_b	CPD	*Meriania albiflora*	Micro-CT	1.000	30.000	200.000	5.080	1.000	3.000	1200.000
CT_152	CPD	*Axinaea grandifolia*	SkyScan	1.000	40.000	175.000	7.000	1.000	0.080	901.000
CT_156_a	CPD	*Meriania calophylla*	Micro-CT	1.000	35.000	200.000	6.770	1.000	1.000	1200.000
CT_156_b	CPD	*Meriania calophylla*	Micro-CT	1.000	35.000	200.000	6.590	1.000	1.000	1200.000
CT_158	EtOH	*Meriania rugosa*	SkyScan	1.000	40.000	175.000	7.000	1.000	0.050	1029.000
CT_165	CPD	*Meriania macrophylla*	Micro-CT	1.000	35.000	200.000	6.100	1.000	1.000	1200.000
FP_001	EtOH	*Meriania haemantha*	SkyScan	1.000	40.000	175.000	7.000	1.000	0.050	1029.000
FP_002	EtOH	*Meriania haemantha*	SkyScan	1.000	40.000	175.000	7.000	1.000	0.050	1029.000

FP_003	EtOH	*Meriania selvaflorensis*	SkyScan	1.000	40.000	175.000	7.000	1.000	0.050	1029.000
FP_004	EtOH	*Meriania selvaflorensis*	SkyScan	1.000	40.000	175.000	7.000	1.000	0.050	1029.000
FP_007	EtOH	*Meriania sanguinea*	SkyScan	1.000	40.000	175.000	7.000	1.000	0.050	1029.000
FP_008_neu	EtOH	*Meriania sanguinea*	SkyScan	1.000	35.000	175.000	7.000	1.000	0.050	1029.000
FP_009	EtOH	*Meriania brachycera*	SkyScan	1.000	40.000	175.000	7.000	1.000	0.050	1029.000
FP_010	EtOH	*Meriania radula*	SkyScan	1.000	40.000	175.000	7.000	1.000	0.050	1029.000
FP_011	EtOH	*Meriania radula*	SkyScan	1.000	40.000	175.000	7.000	1.000	0.050	1029.000
FP_012	EtOH	*Meriania tomentosa*	SkyScan	1.000	40.000	175.000	7.000	1.000	0.050	1029.000
FP_013	EtOH	*Meriania splendens*	SkyScan	1.000	40.000	175.000	7.000	1.000	0.050	1029.000
FP_014	EtOH	*Meriania splendens*	SkyScan	1.000	40.000	175.000	7.000	1.000	0.050	1029.000
FP_015	EtOH	*Meriania mexiae*	SkyScan	1.000	40.000	175.000	7.000	1.000	0.050	1029.000
FP_016	EtOH	*Meriania mexiae*	SkyScan	1.000	40.000	175.000	7.000	1.000	0.050	1029.000
FP_017	EtOH	*Adelobotrys adscendens*	SkyScan	1.000	40.000	175.000	7.000	1.000	0.050	1029.000
FP_018_s	EtOH	*Adelobotrys adscendens*	SkyScan	1.000	40.000	175.000	7.000	1.000	0.050	1029.000
FP_019_l	EtOH	*Adelobotrys adscendens*	SkyScan	1.000	40.000	175.000	7.000	1.000	0.050	1029.000
FP_021_l	EtOH	*Meriania subumbellata*	SkyScan	1.000	40.000	175.000	7.000	1.000	0.050	1029.000
FP_022_l	EtOH	*Meriania subumbellata*	SkyScan	1.000	40.000	175.000	7.000	1.000	0.050	1029.000
FP_023_s	EtOH	*Meriania angustifolia*	SkyScan	1.000	40.000	175.000	7.000	1.000	0.050	1029.000
FP_024_s	EtOH	*Meriania angustifolia*	SkyScan	1.000	40.000	175.000	7.000	1.000	0.050	1029.000
FP_025_l	EtOH	*Meriania angustifolia*	SkyScan	1.000	40.000	175.000	7.000	1.000	0.050	1029.000
FP_026_l	EtOH	*Meriania angustifolia*	SkyScan	1.000	40.000	175.000	7.000	1.000	0.050	1029.000
FP_029	EtOH	*Meriania urceolata*	SkyScan	1.000	40.000	175.000	7.000	1.000	0.050	1029.000
FP_030	EtOH	*Meriania hernandoi*	SkyScan	1.000	40.000	175.000	7.000	1.000	0.050	1029.000
FP_031	EtOH	*Meriania hernandoi*	SkyScan	1.000	40.000	175.000	7.000	1.000	0.050	1029.000
FP_034_l	EtOH	*Meriania calophylla*	SkyScan	1.000	40.000	175.000	7.000	1.000	0.050	1029.000
FP_035_l	EtOH	*Meriania calophylla*	SkyScan	1.000	40.000	175.000	7.000	1.000	0.050	1029.000
FP_037_neu	EtOH	*Graffenrieda maklenkensis*	SkyScan	1.000	40.000	175.000	7.000	1.000	0.050	1029.000
FP_038	EtOH	*Graffenrieda maklenkensis*	SkyScan	1.000	40.000	175.000	7.000	1.000	0.050	1029.000
FP_039	EtOH	*Axinaea alata*	SkyScan	1.000	40.000	175.000	7.000	1.000	0.050	1029.000

FP_040	EtOH	*Axinaea alata*	SkyScan	1.000	40.000	175.000	7.000	1.000	0.050	1029.000
FP_041	EtOH	*Axinaea sclerophylla*	SkyScan	1.000	40.000	175.000	7.000	1.000	0.100	1029.000
FP_042	EtOH	*Axinaea sclerophylla*	SkyScan	1.000	40.000	175.000	7.000	1.000	0.050	1029.000
FP_043	EtOH	*Meriania maguirei*	SkyScan	1.000	40.000	175.000	7.000	1.000	0.100	1029.000
FP_044	EtOH	*Meriania arborea*	SkyScan	1.000	40.000	175.000	7.000	1.000	0.100	1029.000
FP_045	EtOH	*Meriania arborea*	SkyScan	1.000	40.000	175.000	12.000	1.000	0.050	1029.000
FP_046	EtOH	*Meriania inflata*	SkyScan	1.000	40.000	175.000	7.000	1.000	0.050	1029.000
FP_047	EtOH	*Meriania inflata*	SkyScan	1.000	40.000	175.000	7.000	1.000	0.050	1029.000
FP_048	EtOH	*Meriania furvanthera*	SkyScan	1.000	40.000	175.000	7.000	1.000	0.050	1029.000
FP_049	EtOH	*Meriania furvanthera*	SkyScan	1.000	40.000	175.000	12.000	1.000	0.050	1029.000
FP_050_l	EtOH	*Meriania albiflora*	SkyScan	1.000	40.000	175.000	7.000	1.000	0.050	1029.000
FP_051_l	EtOH	*Meriania albiflora*	SkyScan	1.000	40.000	175.000	12.000	1.000	0.050	1029.000
FP_052_s	EtOH	*Meriania albiflora*	SkyScan	1.000	40.000	175.000	12.000	1.000	0.050	1029.000
FP_053_s	EtOH	*Meriania albiflora*	SkyScan	1.000	40.000	175.000	7.000	1.000	0.050	1029.000
FP_054	EtOH	*Meriania maxima*	SkyScan	1.000	40.000	175.000	7.000	1.000	0.050	1029.000
FP_055_l	EtOH	*Meriania maxima*	SkyScan	1.000	40.000	175.000	7.000	1.000	0.050	1029.000
FP_056_s	EtOH	*Meriania maxima*	SkyScan	1.000	40.000	175.000	7.000	1.000	0.050	1029.000
FP_057_s	EtOH	*Meriania maxima*	SkyScan	1.000	40.000	175.000	7.000	1.000	0.050	1029.000
FP_064	EtOH	*Meriania nobilis*	SkyScan	1.000	40.000	175.000	7.000	1.000	0.050	1029.000
FP_065	EtOH	*Meriania nobilis*	SkyScan	1.000	40.000	175.000	7.000	1.000	0.050	1029.000
FP_066	EtOH	*Meriania peltata*	SkyScan	1.000	40.000	175.000	7.000	1.000	0.050	1029.000
FP_067	EtOH	*Meriania crassiramis*	SkyScan	1.000	40.000	175.000	7.000	1.000	0.050	1029.000
FP_068	EtOH	*Adelobotrys macrantha*	SkyScan	1.000	40.000	175.000	7.000	1.000	0.050	1029.000
FP_069	EtOH	*Meriania crassiramis*	SkyScan	1.000	40.000	175.000	7.000	1.000	0.050	1029.000
FP_072	EtOH	*Adelobotrys macrantha*	SkyScan	1.000	40.000	175.000	7.000	1.000	0.050	1029.000
FP_073	EtOH	*Meriania grandiflora*	SkyScan	1.000	40.000	175.000	7.000	1.000	0.050	1029.000
FP_076	EtOH	*Meriania peltata*	SkyScan	1.000	40.000	175.000	7.000	1.000	0.050	1029.000
FP_077	EtOH	*Axinaea wurdackii*	SkyScan	1.000	40.000	175.000	7.000	1.000	0.050	1029.000

FP_078	EtOH	*Meriania longifolia*	SkyScan	1.000	40.000	175.000	7.000	1.000	0.050	1029.000
FP_079	EtOH	*Meriania longifolia*	SkyScan	1.000	40.000	175.000	7.000	1.000	0.050	1029.000
FP_080	EtOH	*Meriania aracaensis*	SkyScan	1.000	40.000	175.000	7.000	1.000	0.050	1029.000
FP_081	EtOH	*Meriania aracaensis*	SkyScan	1.000	40.000	175.000	7.000	1.000	0.050	1029.000
FP_083	EtOH	*Adelobotrys macrantha*	SkyScan	1.000	40.000	175.000	7.000	1.000	0.050	1029.000
FP_084	EtOH	*Meriania hexamera*	SkyScan	1.000	40.000	175.000	7.000	1.000	0.050	1029.000
FP_105	EtOH	*Graffenrieda harlingii*	Micro-CT	2.000	35.000	200.000	3.370	4.000	4.000	1200.000
FP_106	EtOH	*Graffenrieda cucullata*	Micro-CT	2.000	30.000	200.000	2.890	4.000	5.000	1200.000
FP_107	EtOH	*Graffenrieda anomala*	Micro-CT	2.000	30.000	200.000	3.570	4.000	5.000	1200.000
FP_108	EtOH	*Graffenrieda cucullata*	Micro-CT	2.000	25.000	200.000	3.070	4.000	4.000	1200.000
FP_109	EtOH	*Graffenrieda weddellii*	Micro-CT	2.000	30.000	200.000	4.950	4.000	4.000	1200.000
FP_110	EtOH	*Graffenrieda weddellii*	Micro-CT	2.000	30.000	200.000	4.150	4.000	3.000	1200.000
FP_111	EtOH	*Graffenrieda santamartensis*	Micro-CT	2.000	30.000	200.000	2.250	4.000	3.000	1200.000
FP_112	EtOH	*Graffenrieda santamartensis*	Micro-CT	2.000	30.000	200.000	1.930	4.000	3.000	1200.000
FP_113	EtOH	*Graffenrieda harlingii*	Micro-CT	2.000	35.000	200.000	4.050	4.000	6.000	1200.000
FP_114	EtOH	*Graffenrieda colombiana*	Micro-CT	2.000	35.000	200.000	3.370	4.000	5.000	1200.000
FP_118	EtOH	*Graffenrieda colombiana*	Micro-CT	2.000	25.000	200.000	3.370	4.000	3.000	1200.000
M_021_new	CPD	*Meriania rigida*	Micro-CT	1.000	30.000	200.000	7.740	1.000	5.000	1200.000
M_067_new	CPD	*Macrocentrum fasciculatum*	Micro-CT	1.000	35.000	200.000	1.870	4.000	1.000	1200.000
M_068_new	CPD	*Macrocentrum minus*	Micro-CT	1.000	25.000	200.000	1.410	4.000	2.000	1200.000
M_086	CPD	*Meriania paniculata*	Micro-CT	1.000	25.000	200.000	2.010	4.000	1.000	1200.000
M_094	CPD	*Adelobotrys barbata*	Micro-CT	1.000	30.000	200.000	2.450	4.000	2.000	1200.000
M_095	CPD	*Adelobotrys boissieriana*	Micro-CT	1.000	25.000	200.000	2.020	4.000	1.000	1200.000
M_096_b	EtOH	*Adelobotrys macrantha*	SkyScan	1.000	40.000	175.000	7.000	1.000	0.050	1029.000
M_098_a	CPD	*Adelobotrys permixta*	Micro-CT	1.000	25.000	200.000	5.670	1.000	3.000	1200.000
M_100	CPD	*Adelobotrys scandens*	Micro-CT	1.000	30.000	200.000	5.080	1.000	2.000	1200.000
M_101	CPD	*Adelobotrys spruceana*	Micro-CT	1.000	30.000	200.000	5.080	1.000	2.000	1200.000
M_102	CPD	*Adelobotrys tesmannii*	Micro-CT	1.000	30.000	200.000	6.970	1.000	2.000	1200.000
M_112	CPD	*Macrocentrum brevipedicellatum*	Micro-CT	1.000	35.000	200.000	1.260	4.000	4.000	1200.000

M_113	CPD	*Macrocentrum cristatum*	Micro-CT	1.000	30.000	200.000	1.050	4.000	2.000	1200.000
M_116	CPD	*Macrocentrum gesneriaceum*	Micro-CT	1.000	25.000	200.000	1.260	4.000	7.000	1200.000
M_118	CPD	*Macrocentrum neblinae*	SkyScan	1.000	40.000	175.000	*7.000*	1.000	0.080	1029.000
M_119	CPD	*Macrocentrum parvulum*	Micro-CT	1.000	25.000	200.000	1.600	4.000	4.000	1200.000
M_124	CPD	*Maguireanthus ayangannae*	Micro-CT	1.000	30.000	200.000	1.520	4.000	2.000	1200.000
M_127	CPD	*Axinaea scutigera*	Micro-CT	1.000	30.000	200.000	5.080	4.000	4.000	1200.000
M_133	EtOH	*Meriania weberbaueri*	SkyScan	1.000	40.000	175.000	12.000	1.000	0.090	1029.000
M010	EtOH	*Meriania crassiramis*	SkyScan	1.000	40.000	175.000	7.000	1.000	0.050	1029.000
M012	EtOH	*Meriania grandiflora*	SkyScan	1.000	40.000	175.000	7.000	1.000	0.050	1029.000
M014_neu	EtOH	*Meriania hexamera*	SkyScan	1.000	40.000	175.000	7.000	1.000	0.050	1029.000
M016	EtOH	*Meriania longifolia*	SkyScan	1.000	40.000	175.000	9	1.000	0.08	1029.000
M018_lang	EtOH	*Meriania panamensis*	SkyScan	1.000	40.000	175.000	7.000	1.000	0.080	1029.000
M020_neu	EtOH	*Meriania pastazana*	SkyScan	1.000	40.000	175.000	7.000	1.000	0.050	1029.000
M021_neu	EtOH	*Meriania rigida*	SkyScan	1.000	40.000	175.000	7.000	1.000	0.050	1029.000
M045	EtOH	*Graffenrieda rotundifolia*	SkyScan	1.000	40.000	175.000	7.000	1.000	0.080	1029.000
M088a_neu	EtOH	*Meriania peltata*	SkyScan	1.000	40.000	175.000	7.000	1.000	0.050	1029.000
M093_neu	EtOH	*Meriania weberbaueri*	SkyScan	1.000	40.000	175.000	7.000	1.000	0.050	1029.000
M128_neu	EtOH	*Axinaea tomentosa*	SkyScan	1.000	40.000	175.000	7.000	1.000	0.050	1029.000
M129_neu	EtOH	*Axinaea wurdackii*	SkyScan	1.000	40.000	175.000	7.000	1.000	0.050	1029.000
M131_neu	EtOH	*Axinaea floribunda*	SkyScan	1.000	40.000	175.000	7.000	1.000	0.050	1029.000
S09	EtOH	*Meriania hernandoi*	SkyScan	1.000	40.000	175.000	7.000	1.000	0.050	1029.000
S10	EtOH	*Meriania speciosa*	SkyScan	1.000	40.000	175.000	7.000	1.000	0.050	1029.000
S11	EtOH	*Adelobotrys adscendens*	SkyScan	1.000	40.000	175.000	7.000	1.000	0.050	1029.000

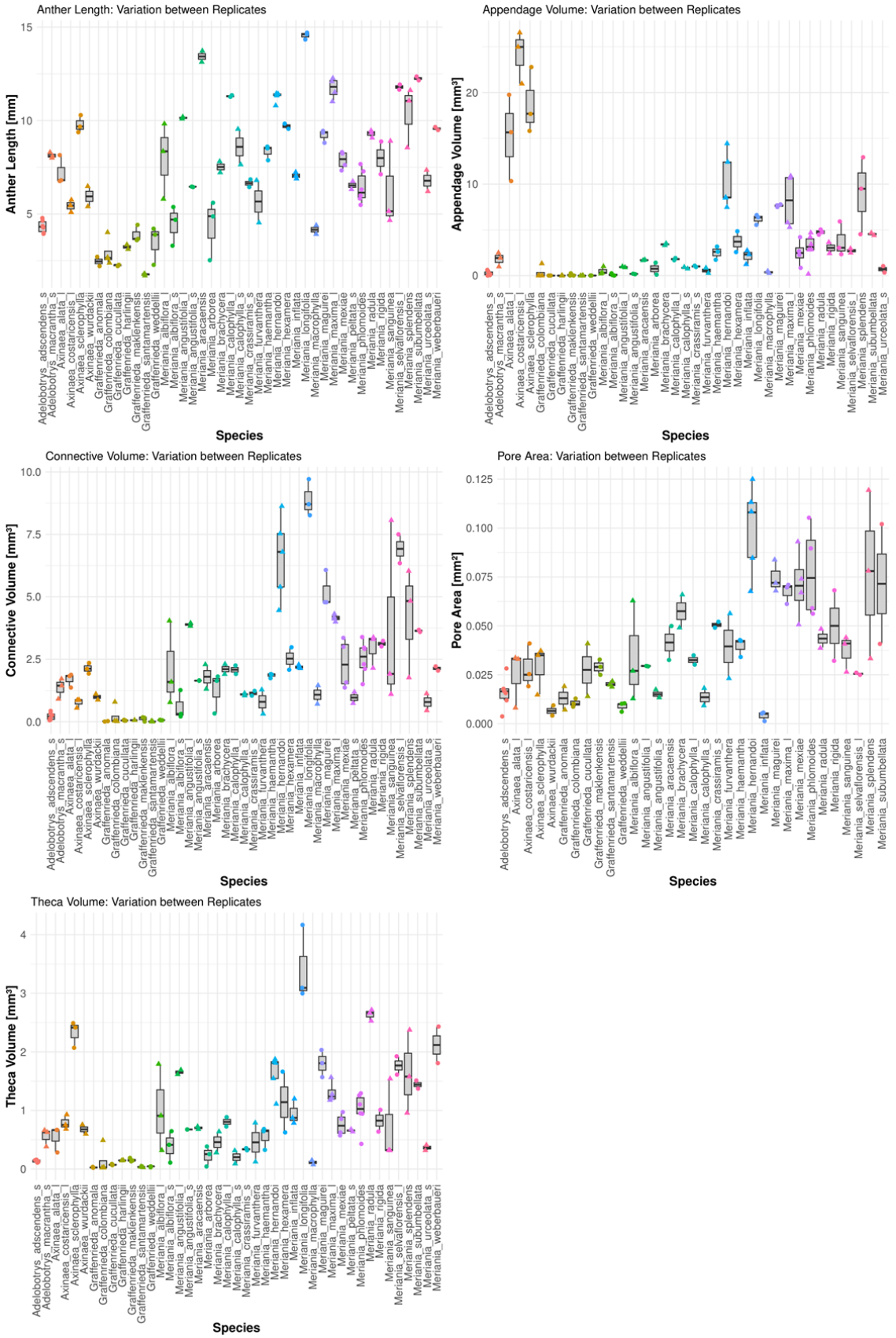

S 2 Boxplots illustrating anther trait values for replicate species. Distinct colors are applied solely to enhance visual clarity

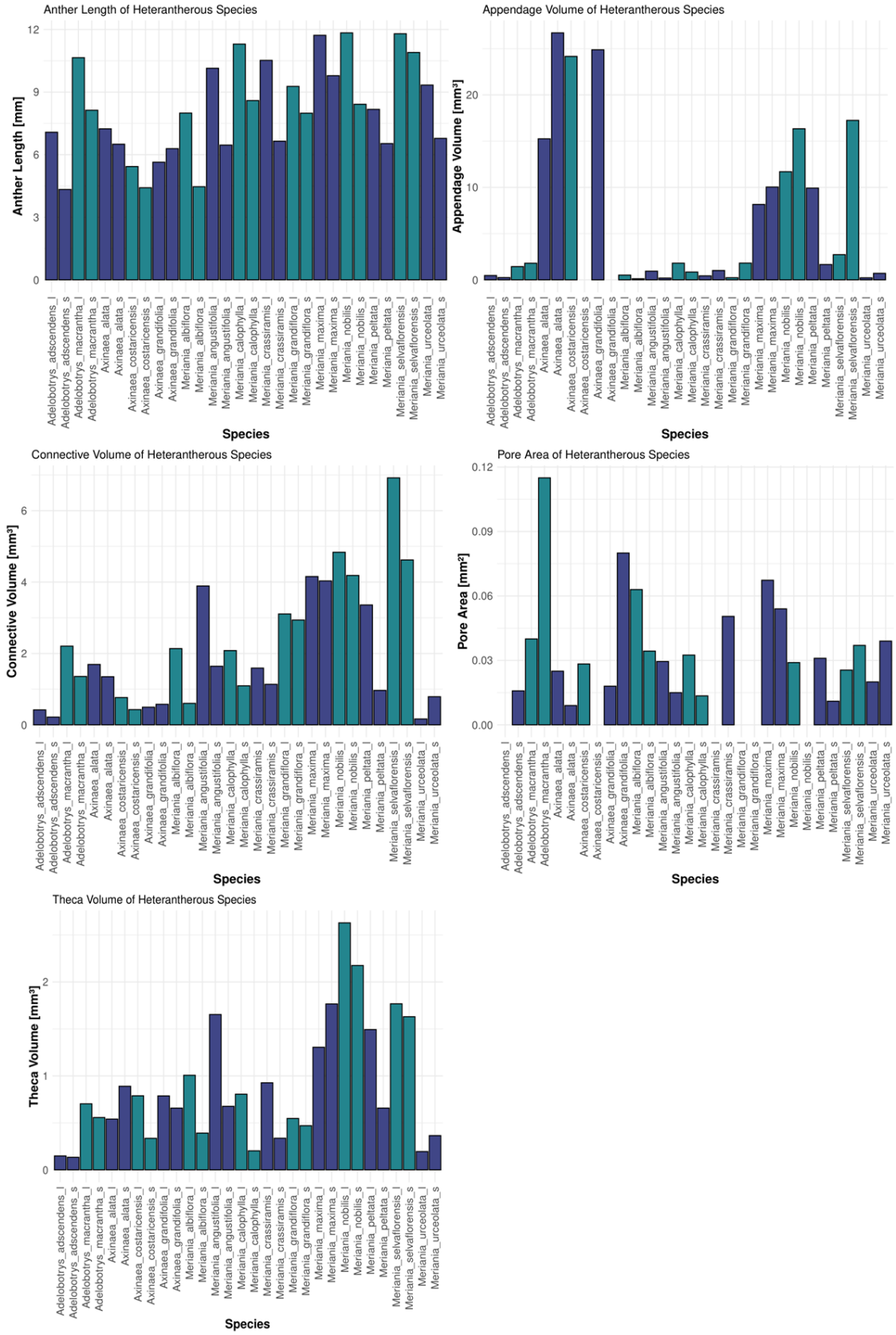

S 3 Bar plots of heterantherous species comparing anther traits between pollinating (l) and feeding (s) stamens. Pairs of bars with the same color represent the same species, while absent bars indicate missing data due to inaccessible measurements.

S 4 Phylogenetic Linear Regression results using the Ornstein-Uhlenbeck (OU) model for elevation.

Phylogenetic Linear Regression using Ornstein Uhlenbeck (OU) model (Elevation)							
Data Set/ Anther Type	Pollination system	value	Anther Length	Appendage Volume	Connective Volume	Pore Area	Theca Volume
Het L/ Pollinating (long)	All	Estimate	0.00080415	0.00272466	0.00089642	1.1776e-05	0.00044707
		P-value	0.06819	0.0003693	0.009114	0.01784	0.003224
		R^2	0.05103	0.201	0.1001	0.1265	0.1258
		Adj. R^2	0.0362	0.187	0.08621	0.1057	0.1124
		AIC	352.8	351.7	289.2	-175.33	212.8
		T-value	1.8551	3.7868	2.6882	2.4657	3.0590
		α	2.00411	0.3337914	0.2556874	2.00411	2.00411
	Bee	Estimate	0.00141787	0.0016306	0.00131137	2.1796e-05	0.00043582
		P-value	0.03096	0.006986	0.000285	0.0007669	0.0005619
		R^2	0.1061	0.1644	0.2663	0.294	0.2441
		Adj. R^2	0.08481	0.144	0.2493	0.2726	0.2265
		AIC	246.5	204.13	194.62	-138.57	100.74
		T-value	2.2327	2.8403	3.9508	3.7068	3.7265
		α	2.00411	0.1210365	2.00411	2.00411	2.00411
Het S/ Feeding (short)	All	Estimate	0.0012186	0.00145249	0.00115095	1.2174e-05	0.00050979
		P-value	0.00927	0.1298	0.001178	0.01602	0.006104
		R^2	0.1278	0.04917	0.1915	0.1304	0.1409
		Adj. R^2	0.1104	0.0285	0.1753	0.1097	0.1237
		AIC	270.8	286	228.8	-174.62	174.32
		T-value	2.7068	1.5424	3.4412	2.5099	2.8637
		α	2.00411	0.1376033	0.345238	2.00411	2.00411
	Bee	Estimate	0.0015069	0.00132900	0.00039599	1.7110e-05	0.00040003
		P-value	0.01753	0.1417	0.3493	0.01152	0.004459
		R^2	0.1469	0.06067	0.02437	0.1888	0.2036
		Adj. R^2	0.1232	0.03383	-0.002731	0.1626	0.1815
		AIC	206.30	205.6	147.69	-125.94	88.13
		T-value	2.4899	1.5035	0.9483	2.6859	3.0341
		α	2.00411	0.1072085	0.04545077	2.00411	0.5270975

S 5 Phylogenetic Linear Regression results using the Pagel's Lambda (λ) model for elevation.

Phylogenetic Linear Regression using Lambda (λ) model (Elevation)							
Date Set (anther type)	Pollination system	value	Anther Length	Appendage Volume	Connective Volume	Pore Area	Theca Volume
Het L/ Pollinating (long)	All	Estimate	-4.9486e-05	0.00166254	0.00031273	1.1776e-05	0.00044575
		P-value	0.9374523	0.09969	0.4324	0.01784	0.003089
		R^2	9.697e-05	0.04684	0.00951	0.1265	0.1269
		Adj. R^2	-0.01553	0.03012	-0.005728	0.1057	0.1135
		AIC	334.4	357.1	288.4	-175.33	212.7
		T-value	-0.0788	1.6736	0.7900	2.4657	3.0737
		λ	0.6354813	0.4953287	0.4179554	3.140294e-07	1e-07
	Bee	Estimate	0.00054087	0.00123788	0.00041881	1.7290e-05	0.00033951
		P-value	0.493285	0.04704	0.3614	0.01987	0.02381
		R^2	0.01125	0.09278	0.01941	0.1537	0.1132
		Adj. R^2	-0.0123	0.07065	-0.003396	0.128	0.09261
		AIC	228.7	206.24	185.89	-139.56	99.96
		T-value	0.6911	2.0476	0.9225	2.4477	2.3432
		λ	0.7163561	0.5046107	0.6598649	0.2547048	0.1781429
	Nectar-foraging-vertebrate	Estimate	-0.0006111	0.00112962	0.00038303	-4.4395e-06	0.00038156
		P-value	0.558479	0.1765	0.7261	0.53633	0.7069
		R^2	0.04451	0.244	0.01619	0.06687	0.01863
		Adj. R^2	-0.07492	0.136	-0.1068	-0.08866	-0.104
		AIC	53.30	41.8	54.36	-36.46	52.86
		T-value	-0.6105	1.5031	0.3629	-0.6557	0.3897
		λ	1e-07	0.1818104	1e-07	1e-07	1e-07
	Passerine	Estimate	-0.00042662	0.0089864	-0.00048970	1.8717e-05	-0.00012095
		P-value	0.66746	0.07259	0.26125	0.1048	0.7221
		R^2	0.01921	0.5072	0.1242	0.2949	0.01321
		Adj. R^2	-0.07886	0.4086	0.0366	0.2068	-0.08547
		AIC	56.08	52.21	35.64	-43.65	30.4
		T-value	-0.4426	2.2684	-1.1908	1.8293	-0.3659
		λ	1e-07	1e-07	1e-07	1e-07	1e-07
Het S/ Feeding (short)	All	Estimate	0.00036412	0.00131891	0.00079811	1.1776e-05	0.00050758
		P-value	0.558625	0.1707	0.04456	0.01784	0.005948
		R^2	0.006887	0.0404	0.07828	0.1265	0.1417
		Adj. R^2	-0.01298	0.01954	0.05984	0.1057	0.1246
		AIC	261.4	293.8	229.2	-175.33	174.30
		T-value	0.5888	1.3917	2.0607	2.4657	2.8733
		λ	0.574999	0.2553523	0.1999375	3.140294e-07	1e-07
	Bee	Estimate	0.00011676	0.00085730	0.0002596	1.4024e-05	0.00023822
		P-value	0.872430	0.3561	0.5263	0.05748	0.1367
		R^2	0.000726	0.02438	0.01125	0.1116	0.06046
		Adj. R^2	-0.02703	-0.0035	-0.01622	0.0829	0.03436
		AIC	190.72	209.2	144.4	-127.28	86.82

		T-value	0.1617	0.9351	0.6399	1.9729	1.5220
		λ	0.7776356	0.4638416	0.9391283	0.1685531	0.2426839
	Nectar-foraging-vertebrate	Estimate	0.00094032	0.00148671	0.0011917	4.3114e-06	0.00072419
		P-value	0.3597	0.05623	0.2888	0.5710	0.4799
		R^2	0.1055	0.4272	0.1389	0.05644	0.06422
		Adj. R^2	-0.006258	0.3454	0.03127	-0.1008	-0.05275
		AIC	52.63	40.6	54.24	-35.48	52.83
		T-value	0.9716	2.2849	1.1360	0.5991	0.7409
		λ	1e-07	1e-07	1e-07	1e-07	1e-07
	Passerine	Estimate	0.0049495	0.0089864	0.00057994	8.0873e-05	0.00093740
		P-value	0.08529	0.07259	0.4428	0.7242	0.05961
		R^2	0.8367	0.5072	0.3104	0.1763	0.8843
		Adj. R^2	0.7551	0.4086	-0.03436	-0.6474	0.8265
		AIC	16.142	52.21	8.7165	-4.534	1.229
		T-value	3.2012	2.2684	0.9489	0.4626	3.9103
		λ	1	1e-07	-0.03436	1e-07	1

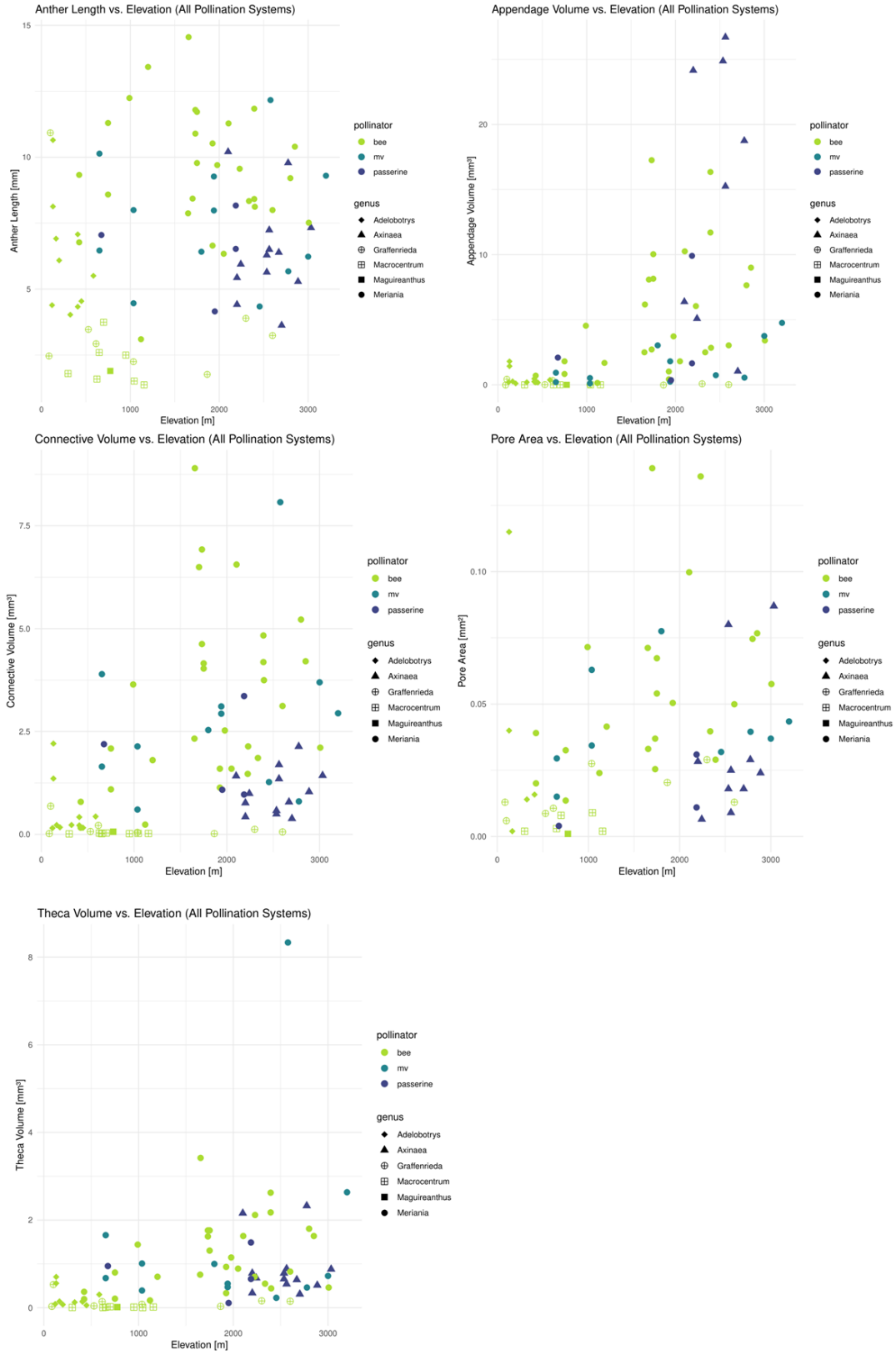

S 6 Scatter plots of anther trait values across all pollination systems plotted against elevation. Pollination syndromes are represented by distinct colors: light green for buzz-bee pollination, blue for nectar-foraging-vertebrate pollination, and purple for passerine pollination. Genera are distinguished by different symbols: rhombus for Adelobotrys, triangle for Axinaea, crossed circle for Graffenrieda, crossed square for Macrocentrum, square for Maguireanthus, and circle for Meriania.

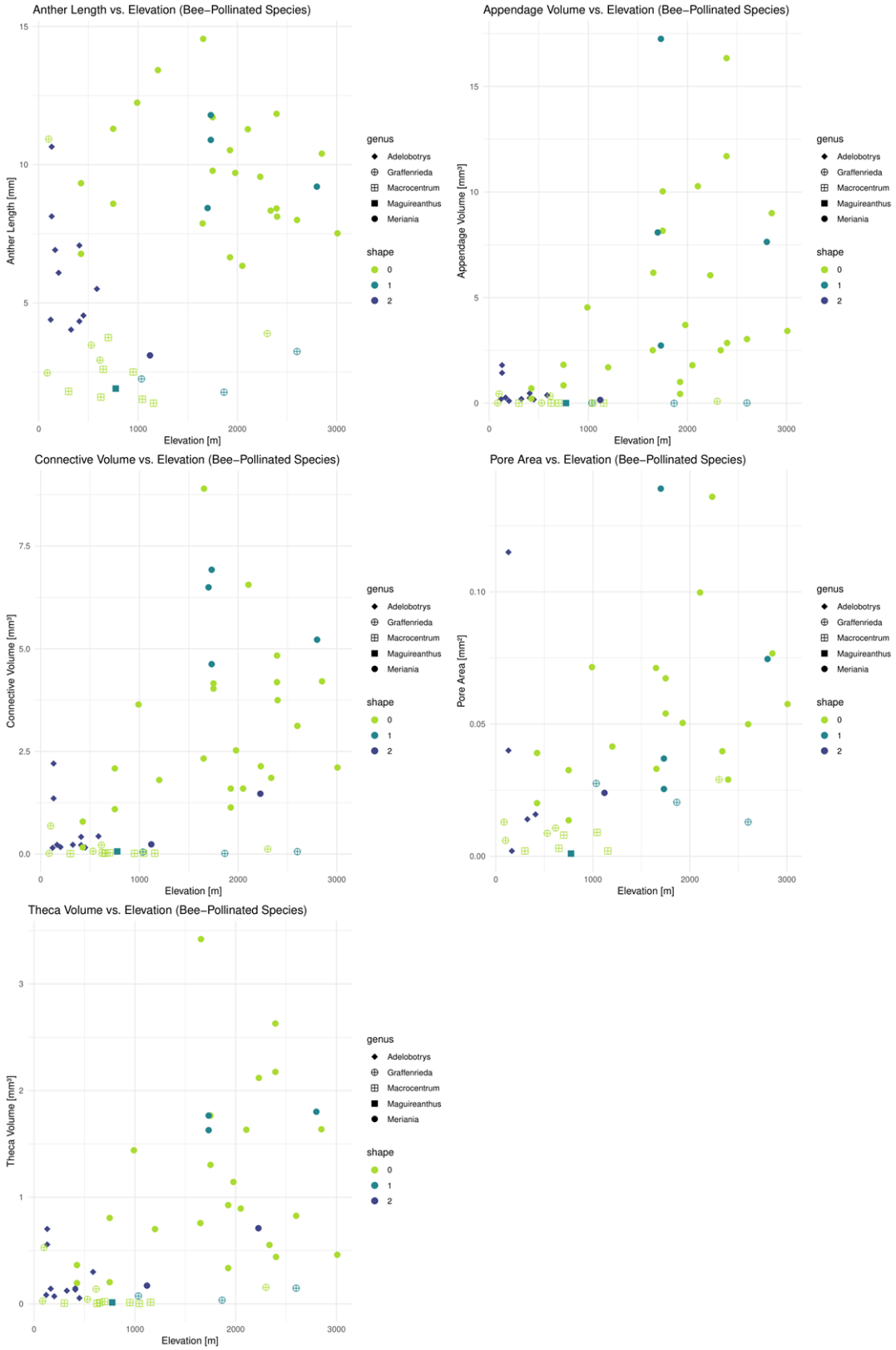

S 7 Scatter plots of anther trait values for bee-pollinated species plotted against elevation. Anther shapes are represented by distinct colors: light green for smooth thecal walls (0), blue for curvy thecal walls (1), and purple for ruminate thecal walls (2). Genera are distinguished by different symbols: rhombus for Adelobotrys, triangle for Axinaea, crossed circle for Graffenrieda, crossed square for Macrocentrum, square for Maguireanthus, and circle for Meriania.